MARMARA UNIVERSITY

INSTITUTE FOR GRADUATE STUDIES
IN PURE AND APPLIED SCIENCES

FABRICATION OF LEVAN-CONTAINING FIBROUS MATRICES

GÜLBEN AVŞAR

MASTER THESIS

Department of Bioengineering

Thesis Supervisor

Prof. Dr. Ebru TOKSOY ÖNER

Thesis CO- Supervisor

Asst. Prof. Oğuzhan GÜNDÜZ

ISTANBUL, 2018

MARMARA UNIVERSITY

INSTITUTE FOR GRADUATE STUDIES IN PURE AND APPLIED SCIENCES

FABRICATION OF LEVAN-CONTAINING FIBROUS MATRICES

GÜLBEN AVŞAR

(524215012)

MASTER THESIS

Department of Bioengineering

Thesis Supervisor

Prof. Dr. Ebru TOKSOY ÖNER

Thesis CO- Supervisor

Asst. Prof. Oğuzhan GÜNDÜZ

ISTANBUL, 2018

MARMARA UNIVERSITY
INSTITUTE FOR GRADUATE STUDIES IN PURE AND APPLIED SCIENCES

Gülben AVŞAR, a Master of Science student of Marmara University Institute for Graduate Studies in Pure and Applied Sciences, defended her thesis entitled "**Fabrication of Levan-Containing Fibrous Matrices**", on Febr 12, 2018 and has been found to be satisfactory by the jury members.

Jury Members

Prof.Dr. Ebru TOKSOY ÖNER (Advisor)
Marmara University .....

Assoc.Prof. Oğuzhan GÜNDÜZ (Co-Advisor)
Marmara University .....

Prof. Dr. Gamze TORUN KÖSE (Jury Member)
Yeditepe University .....

Prof. Dr. Mehmet Ali AĞIRBAŞLI (Jury Member)
İstanbul Medeniyet University .....

Prof. Dr. Faik Nüzhet OKTAR (Jury Member)
Marmara University .....

APPROVAL

Marmara University Institute for Graduate Studies in Pure and Applied Sciences Executive Committee approves that Gülben AVŞAR be granted the degree of Master of Science in Department of Bioengineering, Bioengineering Program on 19.02.2018 (Resolution no: 12345). 2018/06-02

Director of the Institute
Prof. Dr. Bülent EKİCİ

ACKNOWLEDGMENTS

I would first like to thank my supervisors, Prof. Ebru TOKSOY ÖNER and Assoc. Prof. Dr. Oğuzhan GÜNDÜZ for giving me opportunity to perform this thesis, guidance, encouragement and generous support during the development of this study. Thank you for always discussing the results and encouragement after unsuccessful experiments. I would like to thank to Prof. Gamze TORUN KÖSE for her helpful share of HUVECs. Also, I would like to thank Assoc. Prof. Dr. Deniz AĞIRBAŞLI for her technical support. I would also like to thank to my jury committee for giving time to read and evaluate my thesis.

Many thanks to all current and former colleagues that have worked with me in Industrial Biotechnology and Systems Biology (IBSB) research group and Advanced Nanomaterials Research Laboratory. I deeply obliged to Sena SU, Sinem Selvin SELVİ, Burak Adnan ERKORKMAZ, Merve ERGİNER HASKÖYLÜ and Onur KIRTEL for their friendship and being working partners. I would also like to thanks to everyone who was there for me when I need help.

My special thanks to my parents and my brother for their endless patience, deep love and continued support at any time that I felt hopeless and tired. Also, I thank to my partner for his infinite assistance to understand and evaluate the difficulties that comes to my way.

This study was carried out at Marmara University, Department of Bioengineering and Department of Metallurgical and Materials Engineering. In addition, the study has been supported by COST ACTION ENBA CA15216 and The Scientific and Technological Research Council of TURKEY (TUBITAK) through Project 116M838.

January, 2018 **Gülben AVŞAR**

TABLE OF CONTENTS

ÖZET

LEVAN İÇEREN FİBRÖZ MATRİSLERİN ÜRETİMİ

Yaşlanma, hastalanma ve yaralanma gibi nedenler organların veya dokuların fonksiyonlarının yitirilmesine veya azalmasına sebep olabilmektedir. Doku mühendisliği, herhangi bir yetersizliğin meydana geldiği durumlarda organ ve/veya dokuların yenilenmesini ve yeniden oluşturulmasını amaçlayan bir disiplinler arası bilim dalıdır. Doku mühendisliğinde dokusal yenilenmelerin sağlanması için hücrelerin kendilerini doğal yaşam ortamlarındaymış gibi hissetmelerini sağlayan iskele yapıları kullanılır. Canlı vücudunda hücreler, ekstrasellüler matris denilen fibril ve porlu yapılardan oluşan bir ortam içinde bulunur. Hücrelerin doğal yaşamını taklit etmedeki en önemli faktör, aynı topografi ve fonksiyonaliteyi sağlayacak ekstrasellüler matrisi taklit etmektir. Bu nedenle, fibril yapıdaki iskeleler birçok doku mühendisliği uygulamalarında başarılı bir şekilde kullanılabilmektedir. Elektroeğirme yöntemi, hemen hemen her polimere uygulanabilmesi, kolay ve ucuz bir yöntem olması nedenleriyle, fibril yapıda iskelelerin üretiminde en çok tercih edilen tekniktir.

Polisakkaritler, doğal polimerler olmaları nedeniyle birçok biyolojik aktiviteye sahiptirler. Bir homopolisakkarit olan levan, işlevsel bir polimer olarak medikal ve kimyasal endüstride gittikçe yükselen bir popülariteye sahiptir. Ayrıca levanın, suda çözünür, yüksek biyouyumluluğa sahip olması ve biyoyapışkan özelliğinin bulunması onu biyomedikal alanda oldukça çekici hale getirmektedir. Böylece, bu tez kapsamında, levan-kaynaklı fibril yapıları üretilerek levanın biyolojik ortamlardaki avantajlarından yararlanılması ile doku mühendisliği ihtiyaçlarına cevap verecek iskele yapılanın geliştirilmesi hedeflenmiştir.

Bu amaçla, *Halomonas symrnensis* AAD6^{T} bakterisi tarafından üretilen levan polimeri (HL), çözünürlülüğünü artırmak amacıyla hidrolizlenmiştir. Hidrolizlenen polimer (hHL), daha sonra sülfatlama işlemine tabi tutulmuştur. Levan-kaynaklı fibril yapıları için hidrolize levan ve sülfatlanmış hidrolize levan kullanılmıştır. Ayrıca yardımcı polimer olarak polikaprolakton ve polietilen oksit tercih edilmiştir. Fibril üretimi tek-iğneli ve ko-aksiyal elektroeğirme yöntemleri ile gerçekleştirilmiştir. Üretimde kullanılan solüsyonların fiziksel karakterizasyonu ve üretilen fiber matrislerin spektrofotometrik,

morfolojik, mekanik ve biyolojik karakterizasyonları gerçekleştirilmiştir. Ayrıca, sülfatlanmış levan içeren fiberlerin antikoagulasyon aktiviteleri incelenmiştir.

Elektroeğirme yöntemi ile üretilen matrisler, çeşitli çaplarda fibril yapılarına sahip olup fibril bulunurluğu açısından oldukça yoğun bir görünüme sahiptir. Özellikle sülfatlanmış hidrolize levan içeren matrislerin mekanik olarak biyolojik dokulara benzer özelliklere sahip olduğu gözlemlenmiştir. Hidrolize levan içeren matrisler hem fibroblast hem de endotel hücreleri için yüksek biyouyumluluk göstermiştir. Sülfatlanmış hidrolize levan içeren matrisler ise beklenildiği gibi fibroblastların çoğalımını engellerken endotel hücrelerin büyümesini ve çoğalmasını desteklemiştir. Öte yandan, sülfatlanmış hidrolize levanlar içeren fibril iskelelerin antikoagulasyon aktiviteleri incelenmiştir ve sülfatlanmış hidrolize levan konsantrasyonu arttıkça pıhtılaşma süresinin geciktiği gözlemlenmiştir. Bu iki sonuç, özellikle damar doku mühendisliğinde karşılaşılan, yapay damarlarda gerçekleşen tıkanıklık ve endotelleşmenin engellenmesi problemlerinin önüne geçilmesi açısından önem arz etmektedir.

OCAK, 2018 **Gülben AVŞAR**

ABSTRACT

FABRICATION OF LEVAN-CONTAINING FIBROUS MATRICES

Aging, diseases, and injuries can cause to reduce or loss of functions of tissues or organs. Tissue engineering is an interdisciplinary scientific area that aims regeneration and reforming of damaged tissues/organs. Scaffolds are used in tissue engineering applications to support cells with a native host tissue environment. In a living body, cells grow and proliferate in an environment that is called the extracellular matrix with its fibrous and porous structure. The main factor to mimic extracellular matrix is providing an environment that has similar topography and functionality with it. Therefore, fibrous matrices are used for several tissue engineering applications successfully. Electrospinning is the most preferred technique to produce fibrous scaffolds due to being applicable for almost all polymers, easy and inexpensive.

Polysaccharides have various biological activities as natural polymers. Levan that is a homopolysaccharide has an increasing popularity as a functional polymer in medical and chemical industries. Additionally, its water-solubility, high biocompatibility, and bioadhesive properties make levan as an attractive polymer for biomedical applications. Hence, satisfying the needs of tissue engineering by benefiting the advantages of levan in biological environments is aimed at producing levan-based fibrous structures.

Halomonas Levan (HL) that was produced by *Halomonas symrnensis* AAD6^{T} was hydrolyzed to increase its solubility. Then, hydrolyzed *Halomonas* levan (hHL) was exposed to sulfation process. Hydrolyzed *Halomonas* levan (hHL) and sulfated hydrolyzed *Halomonas* levan (ShHL) were used for electrospinning technique, and polycaprolactone and polyethylene oxide were used as helper polymers for single-needle and co-axial electrospinning experiments. The physical characterizations of solutions that were used in electrospinning were determined successfully, and spectrophotometric, morphological, mechanical and biological characterizations of electrospun matrices were performed. In addition, the anticoagulation activity of electrospun matrices that contained ShHL was also investigated.

The produced electrospun matrices had diverse numbers of fiber diameter and a dense fibrillary structure. Especially, ShHL containing fibrous matrices showed similar mechanical properties to the native tissues. High cell proliferation percentage was

observed in both fibroblasts and endothelial cells that were grown on hHL containing fibrous matrices. Fibroblast proliferation was inhibited while endothelial proliferation was supported by ShHL containing fibrous matrices as expected. On the other hand, the anticoagulation activity of ShHL containing fibrous scaffolds was examined, and it was found that the required time for coagulation was increased by increasing concentrations of ShHL. These two results for ShHL have a place in overcoming embolism problem that occurs especially in vascular tissue engineering applications.

January, 2018 **Gülben AVŞAR**

SYMBOLS

cm	Centimeters
g	Gram
h	Hour
kV	Kilovolt
L	Liter
M	Molar
mg	Milligrams
min	Minutes
ml	Milliliters
mm	Millimeters
MPa	Megapascal
mPa.s	Millipascal seconds
nm	Nanometers
s	Second
v/v	Volume per volume
w/v	Weight per volume
µg	Micrograms
µm	Micrometers
µS cm^{-1}	Micro Siemens per centimeters

ABBREVIATIONS

2-(4-amidinophenyl)-1H -indole-6-carboxamidine	DAPI
Attenuated total reflectance	ATR
Blood clotting index	BCI
Dimethylformamide	DMF
Distilled water	dH2O
Dulbecco`s Modified Eagle`s Medium	DMEM
Energy dispersive X-ray	EDX
Extracellular matrix	ECM
Fetal bovine serum	FBS
Fourier transform infrared spectroscopy	FTIR
Glucosaminoglycan	GAG
***Halomonas* levan**	HL
Human umbilical vein endothelial cells	HUVEC
Hydrolyzed *Halomonas* levan	hHL
Polycaprolactone	PCL
Polyethylene oxide	PEO
Scanning electron microscope	SEM
Sulfated hydrolyzed *Halomonas* levan	ShHL
Tetrahydrofuran	THF
Ultimate tensile strength	UTS

LIST OF FIGURES

LIST OF TABLES

1. INTRODUCTION

Human organs are exposed to several changes from their surrounding environment continuously. As a response to that changes, they have ability to maintain their homeostasis. However, loss of functionality is highly possible to occur due to aging, disease and/or injuries. Regenerative sciences use the opportunity of regeneration of organs and tissues with the help of traditional medical treatments, transplantation and alternative novel strategies (Pelipenko, Kocbek, & Kristl, 2015). Tissue engineering and regenerative medicine comprise an interdisciplinary research are that applies chemistry, material science, engineering and medicine. It enables formation of functional tissue by investigating and understanding the deposition, growth and remodeling of tissues (Asghari, Samiei, Adibkia, Akbarzadeh, & Davaran, 2017; Pelipenko et al., 2015) with utilizing three basic tools as cells, biomaterials and biomolecules (Braghirolli, Steffens, & Pranke, 2014). Tissue engineering has been defined as generation of new tissue using engineering principles in modern sciences and was recorded first in 1991 as reported by Vacanti. The birth of this field was in the mid-1980`s by the idea of Dr. Joseph Vacanti and Dr. Robert Langer on designing appropriate scaffolds to generate functional tissue equivalents (Vacanti, 2006). In addition, drug and toxicity testing, and basic tissue development and morphogenesis studies are also included in the field of tissue engineering. Supplying enough cells is a critically important issue that the cells mostly derived from the donor tissue, or stem or progenitor cells. On the other side, the key factor for a functional tissue regeneration is offering an appropriate cellular environment to cells as their native tissue (Berthiaume, Maguire, & Yarmush, 2011).

Studies in tissue engineering has shown that extracellular matrix (ECM) provides mechanical support for cells and, also plays a vital role in regulation of cell behaviors as shown figure 1.1 (F.-M. Chen & Liu, 2016; Pelipenko et al., 2015). With the development of technology novel biomaterials are produced that mimics the native ECM. The scaffold is defined as a device or system that simulates the cells in mechanical and chemical aspects acts as a template for tissue formation (O'brien, 2011), so it should mimic the functions of ECM, at least partially. Firstly, scaffold should be biocompatible that supports cell attachment and growth on it, so rejection of the material

by the host tissue can be minimized. Secondly, scaffold should have a porous structure that enables the transport of nutrients metabolites and cellular penetration, and void volume for vascularization. The pore size should be large enough to allow migration of cells into the structure, but small enough to provide high specific surface area. Thirdly, scaffold should provide an environment for cells to facilitate and regulate their activities. These materials are defined as bioactive that supports cells to have original morphology and alignment. Fourthly, the mechanical properties of scaffold should be similar with the host tissue. A mechanical stability until completion of regeneration is required for scaffolds. Also, stiffness of the scaffold affects the differentiation of stem cells to tissues such as bone, muscle and neuronal (Chan & Leong, 2008; O'brien, 2011).

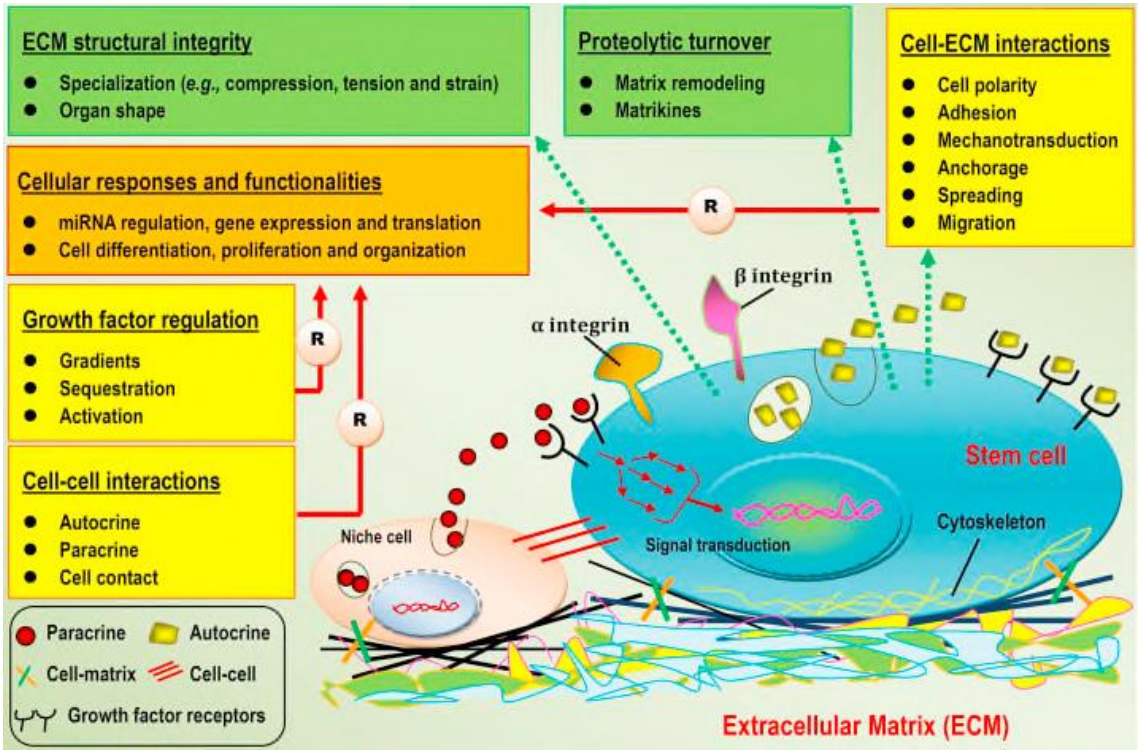

Figure 1.1: Schematic representation of extracellular matrix functions with cell-cell and cell-matrix perspective (F.-M. Chen & Liu, 2016)

The scaffold with fibrous architecture produced by synthetic and/or natural polymers provides desirable properties that counterbalance the requirements of tissue regeneration as mentioned above. Electrospinning is the most commonly preferred scaffold producing technique that used to manufacture consistently nanometric and micrometric fibrous structures (Asghari et al., 2017; Nigam & Mahanta, 2014).

Electrospinning technique is available to be performed with both type of polymeric solutions that are of synthetic or natural polymers. These properties are gained much attention to electrospinning technique in last decades (Bhardwaj & Kundu, 2010). In this study, levan-based fibrous matrices were produced by using electrospinning for tissue engineering applications to investigate and represent the potentials of levan and its derivatives as a biomaterial in fibrous structure. Single-needle electrospinning was used to obtain electrospun matrices that is based on levan and its sulfated derivate by blending them polyethylene oxide. Also, polycaprolactone and sulfated levan were used in co-axial electrospinning technique that polycaprolactone was core polymer where sulfated levan was shell polymer. Then, surface, morphology, mechanical and biological characterizations were performed to investigate the characteristic properties of the electropun matrices.

1.1.Polymers for scaffold production

In general biomaterials are classified in two groups based on their origin that are natural and synthetic polymers (Nigam & Mahanta, 2014). Natural polymers can be represented as protein-origin polymers such as collagen, gelatin, silk fibroin and fibrin, polysaccharidic polymers such as chitosan, starch, alginate, hyaluronan and chondroitin sulfate, and polynucleotides that are DNA and RNA (Malafaya, Silva, & Reis, 2007; Nigam & Mahanta, 2014). Synthetic polymers can be divided as organic polymers such as polycaprolactone, polyethylene oxide, polyvinyl alcohol and polyurethane, and inorganic polymers such as silicone, polyphoshazenes and polysilanes (Manners, 1996; Nigam & Mahanta, 2014). Both have advantages and disadvantages compered to each other. Natural polymers are similar to the host tissue, nontoxic, biocompatible, degradable by enzymes that are in advantages of natural polymers. However, being sensitive to temperature, having a complex structure and possibility of disease transfer by polymer that is derived from plants or animals can be count as disadvantages of natural polymers (Asghari et al., 2017). On the other hand, synthetic polymers have thermal stability and good mechanical properties, so a wide range of shapes can be processed to synthetic polymers (Sionkowska, 2011). However, synthetic polymers do not support cells for attachment and growth on these materials. Hence, the scaffolds that

are combination of both natural and synthetic polymers are considered the best solution for the disadvantages these materials (Nigam & Mahanta, 2014).

1.1.1. Polyethyleneoxide

Polyethylene oxide (PEO) is a biodegradable, biocompatible, non-immunogenic and non-toxic polymer that already have applications in tissue engineering (Ahire, Robertson, van Reenen, & Dicks, 2017; G. Chen, Guo, Nie, & Ma, 2016). It is water soluble polymer that can be dissolved in both cold water and hot water, and also it is soluble in chloroform, ethanol and dimethylformamide (DMF) (Son, Youk, Lee, & Park, 2004). Its melting point is between 63 – 67 ^{o}C and the glass transition is between -50 to -57. The molecular weight of PEO ranges from $1x10^5$ to $8x10^6$ g/mol (Ma, Deng, & Chen, 2014), and the structure is represented in figure 1.2. However, PEO does not show intrinsic bioactivity that supporting protein and biomolecule interaction in vivo, so most of the researchers prefers blending it with bioactive biopolymers (G. Chen et al., 2016). PEO has been approved by the U.S. Food and Drug Administration, so have many applications especially in health and pharmaceutical industries (Knop, Hoogenboom, Fischer, & Schubert, 2010). It has been used in oral controlled release matrix tablets, bioadhesive hydrophilic matrices, osmatic pump tablet systems, thermal insulation and thermal conductivity that depends the filler type, hydrogel forming (Ali, Chipara, Lozano, Hinthorne, & Chipara, 2016; Ma et al., 2014; Xiao et al., 2016). PEO has many applications in tissue engineering such as with chitosan for cartilage (Subramanian, Vu, Larsen, & Lin, 2005), with alginate for skin (Jeong, Krebs, Bonino, Khan, & Alsberg, 2010), and with carboxymethyl cellulose for nerve (Tos et al., 2016) and soft tissue engineering (Basu et al., 2017).

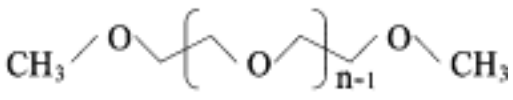

Figure 1.2: The chemical structure of polyethylene oxide (Lee, Venable, MacKerell, & Pastor, 2008).

1.1.2. Polycaprolactone

Polycaprolactone (PCL) is a synthetic polymer which is the most widely used one in bio-applications (Gunatillake & Adhikari, 2003). It is an aliphatic, thermoplastic and biocompatible polymer. This polymer has been used as implantable biomaterial and drug delivery support due to its low melting point and viscoelastic properties. A few products which PCL is used has been approved by the U.S. Food and Drug Administration and has CE Mark (Mondal, Griffith, & Venkatraman, 2016; Woodruff & Hutmacher, 2010). The molecular weight of the polymer varies between 3000 to 80000 g/mol. PCL that the chemical structure is represented in figure 1.3 has a glass transition temperature of -60^{o}C and melting point of 59-64^{o}C (Hayashi, 1994). Mainly ring opening polymerization is preferred to produce PCL by using caprolactone as monomer. Also, many efficient catalysts such as metal catalysis, organic catalysis and enzymatic catalysis are used in the polymerization reaction. Although PCL can be degraded by bacteria and fungi, it is not biodegradable by human and animal due to lack of appropriate enzymes. Therefore, it is resorbed by hydrolysation at *in vivo* conditions and so it takes much longer degradation time (Mondal et al., 2016; Woodruff & Hutmacher, 2010). The semi crystalline structure of PCL provides a slow degradation rate that is almost 2 years (Gunatillake & Adhikari, 2003; Patel et al., 2015). Slow degradation gives advantages for long-term developing tissues and implantable drug delivery systems (Gunatillake & Adhikari, 2003).

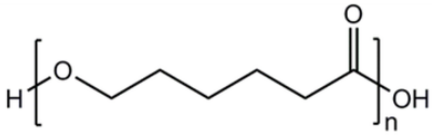

Figure 1.3: The chemical structure of polycaprolactone (Llorens et al., 2013).

The use of PCL has been explored for various tissues such as bone (Hajiali, Tajbakhsh, & Shojaei, 2017), kidney (Burton, Corcoran, & Callanan, 2017), vascular (Abdal-hay, Bartnikowski, Hamlet, & Ivanovski, 2018), cartilage(da Silva et al., 2017), and cornea (Stafiej et al., 2017). There has been an increasing amount of studies that scaffolds have been produces from PCL blending with polysaccharides to increase the bioactivity of the biomaterial for tissue engineering applications such as gelatin for nerve (Ghasemi-Mobarakeh, Prabhakaran, Morshed, Nasr-Esfahani, & Ramakrishna, 2008), chitosan for

retinal (H. Chen et al., 2011), alginate for bone (Kim & Kim, 2014), hyaluronan for skin (Z. Wang et al., 2016), and heparin for vascular (L. Ye et al., 2012) tissue engineering.

1.1.3. Levan

By being natural-based polymers, polysaccharides are mostly bioactive and avoid inflammation and toxicity (Mano et al., 2007). Also, having properties of similarity with extracellular matrix, chemical versatility and high biocompatibility that are curial in biological applications as in tissue engineering (Pina, Oliveira, & Reis, 2015). Natural polysaccharides show fewer side effects, but mostly desired activities cannot be observed because of their inherently physicochemical and structural properties. Thus, some methods are preferred to solve that problem by modifying the structure of polysaccharides. Dimensional structure, the substituent group variety, and positions, the molecular weight can be changed with respect to the performed modification method (S. Li et al., 2016). There are lots of chemical modification methods including sulfation (Erginer et al., 2016; H. Liu, Li, Zhou, Fan, & Fan, 2011), oxidation (Sarilmiser & Oner, 2014; Y. Ye et al., 2017), carboxymethylation (Antosik, Wilpiszewska, & Czech, 2017; Osman, Oner, & Eroglu, 2017), phosphorylation (J. Liu, Luo, Ye, & Zeng, 2012; Oshima, Taguchi, Ohe, & Baba, 2011). Sulfated polysaccharides display various biological activity such as anticoagulant activity (Erginer et al., 2016), anti-oxidant activity (Fimbres-Olivarria et al., 2018), anti-tumor activity (Yu et al., 2017), anti-inflammatory (K. Zhang et al., 2017) and stem cell differentiation (K. Zhang et al., 2017).

Levan is an unusual homopolysaccharide that is composed of beta-(2→6)-fructose monomers as seen in figure 1.4 (Kırtel, Avşar, Erkorkmaz, & Öner, 2017). It is produced by various plants and microorganisms with the fascinating combination of properties. It stands out from other water soluble, biocompatible and film forming biopolymers with its unusual features such as very low intrinsic viscosity, high adhesive strength, health benefits and its ability to gel alcohol (Öner, Hernández, & Combie, 2016). Though known for more than a century, recent efforts to associate its unique properties with high value applications revived the interest in this underexplored polysaccharide and made levan a focus of scientific and industrial interest (Donot, Fontana, Baccou, & Schorr-Galindo, 2012; Freitas, Alves, & Reis, 2011; Öner et al.,

2016). *Halomonas smyrnensis* is an extremophilic bacteria that grows in halophilic environment and produces levan - named *Halomonas* Levan (HL) – with a molecular weight of >1x10^6 Da by using sucrose as a carbon source. Levan is commonly branched that is produced from several bacterial strains such as *Paenibacillus polymyxa* (Han & Watson, 1992), *Microbacterium laevaniformans* (Oh, Yoo, Bae, Cha, & Lee, 2004), *Gluconacetobacter diazotrophicus* (Hernandez et al., 1995), *Zymomonas mobilis* (Calazans, Lopes, Lima, De Franc, & others, 1997). Unlike the mentioned bacterial, *H. smyrnensis* produces unbranched linear levan (Öner et al., 2016). High yield production of HL provides industrially importance by low-cost production due to the advantage of the unsterile process of halophilic fermentation broth (Sarilmiser, Ates, Ozdemir, Arga, & Oner, 2015). As a water soluble, biocompatible and film-forming polymer, HL has distinguishing properties such being anti-oxidant (Kazak et al., 2014) and anti-cancer (Sarilmiser & Oner, 2014). Also, previous studies demonstrated its potential uses as drug carries in nano and micro forms (Sezer et al., 2017; Sezer, Kazak, Öner, & Akbu\uga, 2011), multilayer adhesive films (Costa et al., 2013), blend films (Bostan et al., 2014), temperature responsive hydrogels (Osman et al., 2017) and nanostructured bioactive surfaces by laser deposition (Axente et al., 2014; Sima et al., 2012). In addition, its sulfated derivative (ShHL) showed dose dependent heparin mimetic activity with its high biocompatibility that makes it suitable for functional biomaterial in designing engineered smart scaffolds (Erginer et al., 2016).

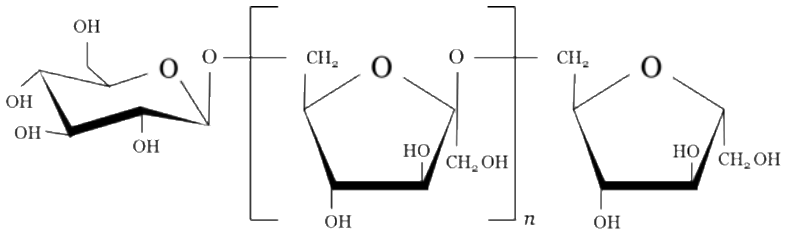

Figure 1.4: Chemical structure of *Halomonas* levan

Sulfated polysaccharides can be obtained naturally or chemically synthesized. Many studied reported that sulfated polysaccharides show stronger biological activity (Y. Lu, Wang, Hu, Huang, & Wang, 2008), high antiviral (Ghosh et al., 2008), anticoagulant and antiplatelet coagulation (Alban, Schauerte, & Franz, 2002), and antioxidant activities (Alban et al., 2002).

1.1.4. Heparin mimicry

Heparin is a widely used sulfated polysaccharide as a lifesaving drug with the properties of anticoagulant by binding antithrombin and heparin cofactor II that provides inactivation of enzymes responsible for coagulation (Casu, Naggi, & Torri, 2015; Nogueira, Drehmer, Iacomini, Sassaki, & Cipriani, 2017). Heparin belongs to glycosaminoglycan family and has a linear structure that consists of 1→4 linked disaccharide sequences of glucosamine and uronic acid residues as seen figure 1.5 (Liang & Kiick, 2014). It has an average molecular weight of ~17-19 kDa that purified from bovine or porcine tissues (Groner, Ng, Wang, & Udit, 2015). The sulfate that is found in the structure with an average of 2.7 sulfates per disaccharide repeats provides a high negative charge to heparin. This negative charge mediates electrostatic interactions with various proteins such as growth factors, chemokines and proteases. This interaction provides stabilization of proteins and increases the affinity of proteins for cell receptors (Groner et al., 2015; Liang & Kiick, 2014). It is known that heparin has a tendency to bind specifically vascular endothelial growth factor (VEGF) and basic fibroblast growth factor (FGF) that are angiogenic growth factors (Spadaccio et al., 2010).

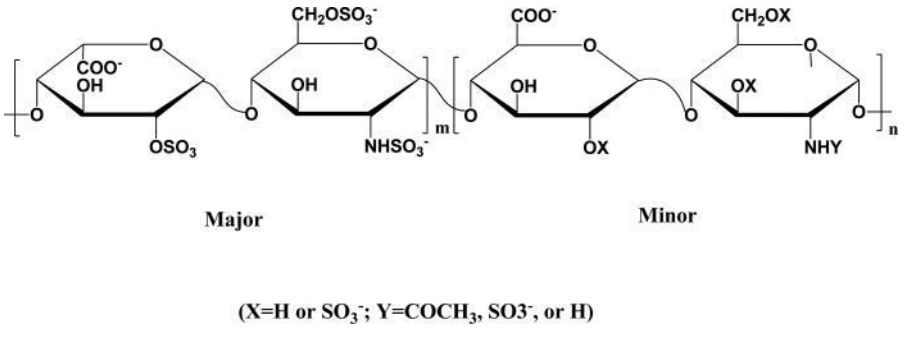

Figure 1.5: Structure of heparin with major (85%) and minor (15%) (Liang & Kiick, 2014).

Besides the using of heparin as a drug, heparin-conjugated materials are seen as good candidates for anti-coagulation of blood-contacting biomaterials (L. Ye et al., 2011). On the other side, heparin has known to inhibit the proliferation of many kinds of cells such as fibroblasts, vascular smooth muscle cells and mesangial cells (F. Chen, Huang, & Mo, 2010). Guyton and his team studied arterial smooth muscle cell proliferation by heparin and showed that heparin inhibits smooth muscle cell proliferation and inhibition

is not mediated by effects on other cells or by antithrombin (Guyton, Rosenberg, Clowes, & Karnovsky, 1980). Loung-Van and his co-workers also reported the inhibition of smooth muscle cell proliferation by using polycaprolactone electrospun nanofibers that were blended with heparin (Luong-Van et al., 2006). The fibers that released heparin reduced the net cell growth with a ratio of 40% compared to heparin-free control groups. In addition, inhibition of fibroblast cells by heparin was proved by Del Vecchio by using scleral fibroblasts for ocular trauma and surgical wound healing (Del Vecchio, Bizios, Holleran, Judge, & Pinto, 1988). The proliferation of fibroblasts (2.6 doublings) that was treated with heparin was lower than proliferation of non-treated control groups (4.9 doublings) with a ratio of nearly 50 percent. Beside levan-based biomaterials, these findings lead to consider of investigation the usage of levan sulfate that has heparin-like activity as an anticoagulation agent for blood-contacting biomaterials. The chemical structure of sulfated *Halomonas* levan is represented in figure 1.6.

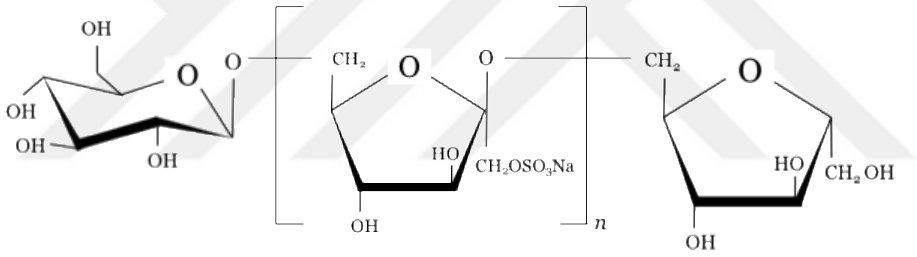

Figure 1.6 : The chemical structure of sulfated *Halomonas* levan

1.2.Techniques for scaffold production

Scaffolds are the biomaterials that can be produced from synthetic polymers, natural polymers and ECM molecules by using several techniques that some of them are shown in figure 1.7 (Nigam & Mahanta, 2014). In tissue engineering applications, scaffolds should be biodegradable, biocompatible, nontoxic, non-mutagenic and non-immunogenic (Asghari et al., 2017; Bacakova, Novotná, & Parizek, 2014). Mimicking porous structure of ECM is the most important key factor to be a functional scaffold that supports an environment to the cell similar to native tissue. The scaffolds that are produced by hydrogels, electrospinning, gas-foaming, salt leaching and freeform fabrication techniques shows similarities to native ECM.

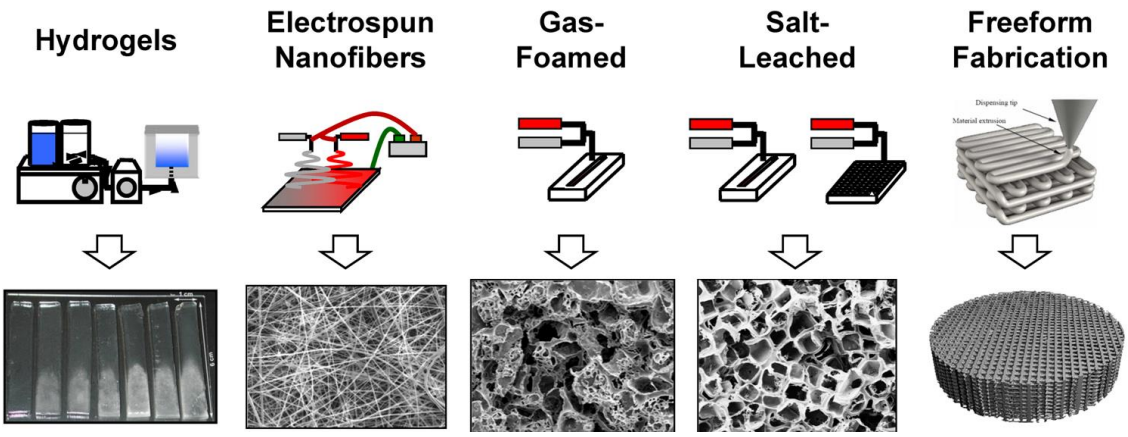

Figure 1.7: Different methods using for fabrication of scaffold (Nigam & Mahanta, 2014).

Hydrogels are polymer networks that are crosslinked chemically or physically. They are defined as water-swollen due to the capability of absorbing large amounts of water. Various parameters that are preparation method (homopolymer, or copolymer hydrogels), mechanical and structural characteristics (amorphous, semicrystalline, hydrogen-bonded, supramolecular, or hydrocolloidal), and the overall charge (neutral, anionic, or cationic) are used in the classification of hydrogels (Van Vlierberghe, Dubruel, & Schacht, 2011). Hydrogels are attractive especially for drug delivery and regeneration of soft tissues due to their characteristic properties. However, difficulty to shape into predesigned geometries and low mechanical strength are the main disadvantages of hydrogels (Billiet, Vandenhaute, Schelfhout, Van Vlierberghe, & Dubruel, 2012).

In gas foaming technique, the melted polymer is exposed to gases such as N_2 and/or CO_2 at high pressure to blow the polymer physically then the pressure is increased to atmospheric pressure. Hence, an interconnected porous structure is formed that cells can migrate and transport of biomolecules can occur (Sachlos, Czernuszka, & others, 2003). Due to avoiding from organic solvent usage, gas foaming has advantages to provide nontoxic environment compared to organic solvents. However, difficulties in processing due to rheological and mechanical properties are the main disadvantages of gas-foaming technique. (Salerno, Netti, Di Maio, & Iannace, 2009).

The polymer solution is mixed with a water-soluble salt such as sodium chloride or sodium citrate particles, and the desired shape for scaffold is obtained by using molds

in salt leaching technique. After evaporation or lyophilization of solvent, the salt particles are leached out. Hence, a porous structure is obtained with the desired scaffold shape. Salt leaching technique has many advantages of simplicity of processing and controlling pore size and pore number by controlling salt size and salt concentrations. However, the shape of pore must be in cubic crystal salt geometry. Also, the thickness of the scaffold should be low to allow removing of salt particles (Hou, Grijpma, & Feijen, 2003; X. Liu & Ma, 2004).

Selective laser sintering, stereolithography and 3D printing are the examples of freeform fabrication that the material or energy is delivered sequentially (Nigam & Mahanta, 2014). This layer-by-layer additive manufacturing allows constructing scaffolds that internal and external geometrical properties are controlled (Williams et al., 2005). Selective laser sintering is a rapid prototyping technique that the desired shape is defined computationally. A bed of powder is used in selective laser sintering technique. When the laser scans the surface of the powder bed, the temperature is increased and the powders fuse together. This method is rapid and easy to use (Williams et al., 2005). However, some polymers decompose under laser instead of fusing and high energy comes by the laser may cause the increase in mechanical properties at the final parts that result in inaccurate dimensions in the final structure (Shirazi et al., 2015). Stereolithography based on photopolymerization of photosensitive monomer resin by UV radiation. The scan of UV light on the resin surface provides a thin structure based on the defined shape computational, then the process continues until final scaffold is obtained (Bikas, Stavropoulos, & Chryssolouris, 2016; Mota, Puppi, Chiellini, & Chiellini, 2015). Stereolithography provides the advantage of not using a support material, and it is rapid and easy to produce scaffolds. However, UV light intensity can induce polymer degradation, the mechanical strength of the obtained scaffold is mostly low, and control of surface topology is poor with stereolithography (Mota et al., 2015). 3D printers use inject printing technology that contains powder supply and a binder print head. The polymerization of monomers that are in powder form is achieved by the binder that is supplied with a head (Bikas et al., 2016). The 3D printers that are used in tissue engineering are generally based on extrusion of the polymer. Extrusion-based systems use motor acquitted plunger or pneumatic to deposit the polymer layer-by-layer. The system is calibrated for each polymer by adjusting nozzle size and nozzle geometry,

and deposition rate. In addition, 3D printers allow cells to be deposited with or without polymers for production of 3D structures that is called 3D bioprinting (Sears, Seshadri, Dhavalikar, & Cosgriff-Hernandez, 2016). The 3D printer provides high production rate (Mota et al., 2015). However, the main disadvantage of 3D printing is short solidifying time for deposited polymers. The polymer should be liquid to be able to extrude from the nozzle, and after extrusion, the polymer should be solidify rapidly to get the desired shape that is predefined (Sears et al., 2016).

Electrospinning is a method that produces polymeric fibers by using high voltage supply to evaporate the solvent while nanometric and micrometric polymer fibers occur (Asghari et al., 2017). It provides ECM-like structure by providing dense fibers, tunable porosity and adjusting fiber composition (Bhardwaj & Kundu, 2010). The details of electrospinning methods have been explained in section 1.3.2.

1.2.1. Fibrous scaffold production methods

The main idea of scaffolding is to mimic the native ECM to provide a natural environment for cells to obtain functional tissue. Fibers can mimic the natural ECM to provide cell support results having great potential to produce biomedical scaffolds (Repanas, Andriopoulou, & Glasmacher, 2016). Polymeric nanofibers are promising materials due to not only ECM structure similarity but also their mechanical properties (Pelipenko et al., 2015). They have a curial role in tissue engineering through cell seeding, proliferation, and new tissue formation (Asghari et al., 2017). Therefore, polymeric materials in fibrous structure are one the most preferred scaffold to mimic ECM and support tissue regeneration.

Phase separation, self-assembly and electrospinning are the techniques that are used to produce fibrous structure for tissue engineering applications, and the schematic representation is shown in figure 1.8. In phase separation technique, polymer is dissolved in a solvent, then thermal-cooling or non-solvent exchange that induces the gelation is performed. Therefore, polymer rich phase occurs. The solvent is replaced by water and then scaffold is frozen for lyophilization. This technique produces fibrous scaffold that the fiber diameter is changed between 50 to 500 nm (Wade & Burdick, 2012, 2014). Self-assembly is a spontaneous process that is molecules (such as peptides and proteins) forms ordered fibrillary structures through several interactions such as van

der Waals interactions, electrostatic interactions, hydrogen bonding, and hydrophobic interactions (Smith, Liu, & Ma, 2008). This process is initiated by mixing two molecules or an external stimulus such as pH, ionic strength and temperature (Wade & Burdick, 2014).

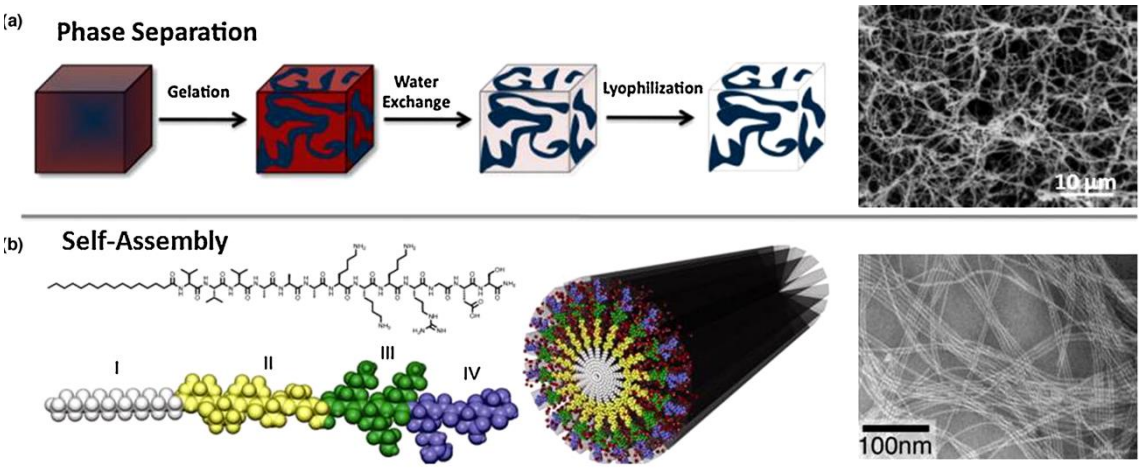

Figure 1.8: Schematic of fibrous structure production techniques used in tissue engineering applications. a) phase separation technique and b) self-assembly technique (X. Wang, Ding, & Li, 2013).

1.2.2. Electrospinning method

Electrospinning (electrostatic fiber spinning) (Mirjalili & Zohoori, 2016) is the most widely preferred technique to construct fibrous biomaterials. It provides continuous fibers with different scales from nanometres to wider dimensions. This technique catches the eyes of both academia and industry by being able to apply for various materials such as natural and synthetic polymers. The first studies for this technique were in 1745s (Braghirolli et al., 2014), and the first patent recorded in 1934 by Anton who introduced an apparatus to produce polymeric filaments by electrostatic repulsions between surface charges of polymer solution and collector (Anton, 1934). Until 1990s, there was no interest to manufacture biomaterials commercially with the technique of electrospinning (Braghirolli, Steffens et al. 2014). In recent years, electrospinning studies have grown exponentially with its various application areas, ability to produce complex constructions and improving the mechanical properties.

Electrospinning uses an electrical field to produce fine polymeric fibers. The technique is simple and inexpensive. Basically, the machine comprises three components; a spinet with a pump, a collector and a high voltage supplier as seen figure 1.9. As a spinet, small diameter metal capillary needle is generally preferred. High voltage causes a jet of polymer solution that travels from spinet to collector. Before reaching the collector, solvent in the jet evaporates and fibers are collected. The electrical field is applied through both the electrode into the solution and the collector. Increasing the field causes hemispherical shape at the tip of the syringe. Then this hemispherical shape creates a cone that is called Taylor cone. With high electrical field, electrostatic force overcomes the surface tension of polymer solution that causes the elongation of Taylor cone means a jet is created towards the collector. The jet moves a certain distance in a straight way, then it moves in a spiral path. Evaporation of solvent occurs on the path because of jet instability and tension (Asghari et al., 2017).

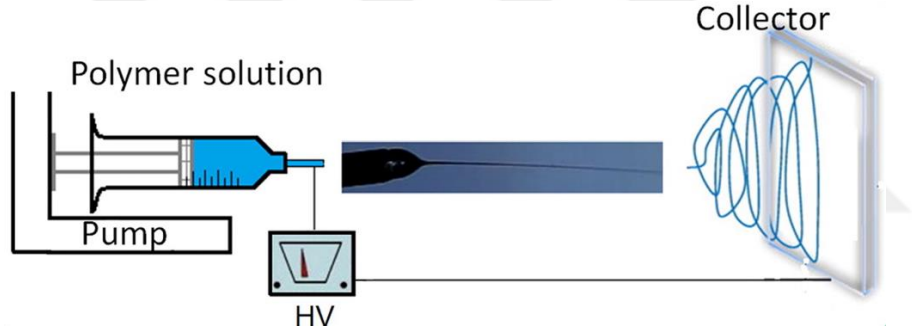

Figure 1.9: Schematic representation of electrospinning method (Pelipenko et al., 2015).

Electrospinning process is affected by solution parameters, process parameters and ambient parameters (Z. Li & Wang, 2013). Solution viscosity and surface tension are critical keys for fiber morphology. The formation of droplets or particles have occurred with tendency of surface tension to reduce the surface area per unit mass. Polymer jet to smooth fibers occurs when viscoelastic forces promote (Kong & Ziegler, 2013). The concentration of polymer solution influences the stretching of charged jet. When polymer concentration is very low, polymer chains break into fragments and electrospray occurs due to low viscosity and high surface tension of the solution (Haider, Haider, & Kang, 2015; Z. Li & Wang, 2013). At the appropriate concentration, smooth fibers can be observed. If the concentration is very high, helix-shaped micro-ribbons will be obtained (Z. Li & Wang, 2013). Solution conductivity meanly influences the

Taylor cone formation which is essential to get a polymer jet. If conductivity is low, Taylor cone does not occur and so electrospinning cannot be performed (Haider et al., 2015). And until a critical point, increasing the conductivity also causes decrease of fiber diameter (Haider et al., 2015; B. Sun et al., 2014). The role of solvent is also important for electrospinning method. Two things need to be paid attention to solvent selecting. First, the polymer should be dissolved completely in the preferred solvent. Second, the boiling point of the solvent should be appropriate due to solidification with very low boiling point and non-solidification during spinning with very high boiling point (Haider et al., 2015; Sill & von Recum, 2008; B. Sun et al., 2014).

Electrospinning has many advantages by being easy to use. However, the process parameters such as applied voltage, flow rate, collector-tip distance highly affect the result of the process. The applied electrical field is important to achieve Taylor cone and form the jet by electrostatic repulsive forces on the fluid jet (Okutan, Terzi, & Altay, 2014; Sill & von Recum, 2008). The applied voltage also has a role in fiber diameter that increasing the voltage results in decrease in nanofiber diameters. High voltages cause high dimeters of fibers, and bead formation can be observed with very high voltages (Okutan et al., 2014). Flow rate of polymer solution influences the fiber diameter. To get enough polymerization between tip and collector, low flow rate is generally recommended. High flow rates cause the fibers with large diameters and bead formation (Haider et al., 2015; Sill & von Recum, 2008). The distance between collector and tip is also one of the parameters, which influence the fiber diameter and morphology. The solidification of the polymer solution will not have enough time with too short distance. Therefore, very thick fibers or non-porous matrices will occur. Generally increasing the distance results in decrease the fiber diameter. Also, if the distance is too long, fibers cannot occur (Haider et al., 2015; Sill & von Recum, 2008).

The ambient parameters such as temperature and humidity also affect the fiber diameter and morphology. Increasing the temperature results in thinner fibers, whereas viscosity will also decrease. This inverse relationship forces the process to be carried out in critical ranges of temperature and viscosity. Low humidity leads the rapid drying of the solvent, so it favors thinner fiber diameters (Bhardwaj & Kundu, 2010; Haider et al., 2015). As also pointed out for levan by Manandhar and coworkers (Manandhar, Vidhate, & D'Souza, 2009), biopolymers are usually soluble in aqueous solutions which

in turn generates difficulties in forming homogeneous fibers due to their poor molecular flexibilities, being polyelectrolytes when dissolved and most importantly due to insufficient entanglement (Drosou, Krokida, & Biliaderis, 2017; J.-W. Lu, Zhu, Guo, Hu, & Yu, 2006). Therefore, using a fiber-forming polymer as a template is the most preferred technique for electrospinning to overcome these difficulties (Drosou et al., 2017; J.-W. Lu et al., 2006; Y. Z. Zhang, Su, Ramakrishna, & Lim, 2007).

The improvement of quality and the functionality of the produced fiber matrices is the main reason that various modifications have been done in the basic electrospinning process. One of these modifications which is called co-axial electrospinning (also called two-fluid electrospinning) has gained much attention by having similar set-up process with basic electrospinning. The technique was first reported by Loscertales et al. (Loscertales et al., 2002) in 2002 with produced capsules in electrospraying method. And it is developed under the name of co-electrospinning by Sun et al. (Z. Sun, Zussman, Yarin, Wendorff, & Greiner, 2003) in 2003 with produced nanofibers in core-shell structure. A modification in the spinneret is done for co-axial electrospinning. A thinner capillary is set in the bigger capillary as shown in the figure 1.10. In this process, two different polymer solutions are derived from the co-axial spinneret independently. When the polymer solutions are charged due to applied high voltage, the Taylor cone appears and a jet that contains both polymers occurs. Because the method is similar to conventional electrospinning technique, all mentioned before parameters also affect the co-axial electrospinning process (Elahi, Lu, Guoping, & Khan, 2013; Moghe & Gupta, 2008). Co-axial electrospinning technique can also be preferred when the shell solution is not able to electrospinnable (Sultanova, Kaleli, Kabay, & Mutlu, 2016).

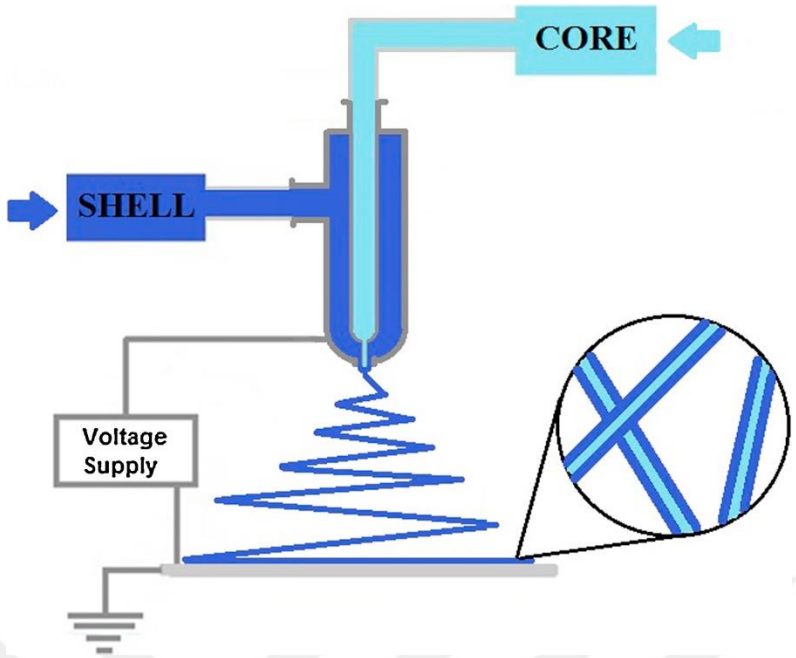

Figure 1.10: Schematic of co-axial electrospinning (Sultanova et al., 2016).

Electrospun fibers are suitable candidates for biomedical and drug delivery applications by having important properties such as high porosity, adjustable pore size, high surface-to-volume ratio, and morphological similarity to ECM. On the other hand, electrospun fiber matrices have applications increasingly in tissue engineering scaffolds, wound dressings for healing, filtration processes, biosensor systems, protective clothing, energy generations, immobilization of enzymes, affinity membranes and cosmetics (Bhardwaj & Kundu, 2010).

Electrospun matrices have advantages with their very small pore size in the filtration industry. Kang *et al*. (Kang & Kang, 2016) used zeolite in polymeric solution to produce an electrospun fiber matrices which can perform both filterings out the dust particles and dehumidification. They found that the films with polyvinylidene fluoride and zeolite have potential to manufacture cost effective filtering material. Ramos *et al*. (Ramos, Morales, Goyanes, Candal, & Rodr'\iguez, 2016) produced humidity sensor with polyvinyl alcohol and multi-walled carbon nanotubes by taking advantages of high area/volume ratio of electrospun matrices. Some functionalization operations with of multi-walled carbon nanotubes tend to damage the structure. However, Ramos and his group achieved this problem with the used electrical field of electrospinning method by carbon nanotube deposition onto the surface of the polymer. Yao *et al*. (Z.-C. Yao,

Chang, Ahmad, & Li, 2016) preferred coaxial electrospinning of rose hip seed oil and zein prolamine for food preservation. They directly covered the electrospun films onto fruits and observed for 7 days. The results showed that electrospun packaging improved food sustainability and reduced waste.

Shao and his group (Shao et al., 2016) worked on bone tissue engineering by preparing multilayer electrospun fabric. They reported that the scaffolds provided mesenchymal stem cell adhesion and proliferation. And in vivo new bone formation was also reported with biomimetic architecture, high biocompatibility and good mechanical properties. Electrospun fibrous matrices have high potential for wound healing that was proved by Vigneswari and his group (Vigneswari, Murugaiyah, Kaur, Khalil, & Amirul, 2016). P(3-hydroxybutyrate-co-4-hydroxybutyrate) and collagen peptides were used as polymer solution in electrospinning process using dual syringe system. The electrospun fibrous matrices showed highest wound closure with a percentage of 79% in animal tests by mimicking the natural tissue.

Sultanova et al. (Sultanova et al., 2016) produced core-shell fibers which were ampicillin loaded to provide controlled release of drug. The drug release kinetics of core-shell products was observed closer to zero-order kinetics while serious burst release was showed by the drug release kinetics of single electrospinning products. Immobilization of cyclodextrin glucanotransferase which is industrially important was performed by Saallah et al. (Saallah et al., 2016). They applied co-electrospinning with a single spinneret by using polyvinyl alcohol with enzyme. The enzyme immobilization with electrospinning showed nearly 2.5-fold higher enzyme loading and 31% higher enzyme activity in compression with film.

2. MATERIALS AND METHODS

2.1.Materials

Halomonas levan (HL) was produced by microbial fermentation under controlled bioreactor conditions and purified as reported before (Poli et al., 2009; Sarilmiser et al., 2015). Polycaprolactone (PCL, Mw=80,000) and polyethyleneoxide (PEO, Mw=300,000), and solvents tetrahydrofuran (THF) and dimethylformamide (DMF) were purchased from Sigma-Aldrich (Poole, UK).

2.2.Laboratory equipment

Analytic Balance (252 g / 0.1 mg)	: AND A&D Company Limited, Japan
Autoclave (Mod3870 Elv)	: Systec, Germany
Automatic Pipettor Sets (Research plus)	: Eppendorf, Germany
Centrifuge (Z36HK)	: Harmle, Germany
Centrifuge (NF 800)	: Nüve, Turkey
Deepfreezes (-80 °C)	: Heto Holten, Denmark
Freezer (-20 °C)	: Arçelik, Turkey
Refrigerator (4°C)	: Arçelik, Turkey
Heating Magnetic (StirrerMr3003s)	: Heidolph,Germany
Laminar Flow Cabinet (MN 090)	: Nüve, Turkey
Ovens (Oven Bd115)	: Binder, Germany
pH Meter (Mp 220k)	: Mettler Toledo
Spectrophotometer (UV/Vis, Lambda35)	: Perkin Elmer
Vortex	: Heidolph, Germany
Water Purification Systems	: Elga PURELAB, UK
T25 and T75 Cell Culture Flasks	: TPP, USA
Disposable Pipette (5, 10, 25 ml)	: TPP, USA

Well Plates (6, 12. 24, 96)	: TPP, USA
Inverted Light Microscope	: SOIF XDS-IB, Turkey
Sterile Incubator (USA)	: Thermo Scientific Steri-cycle CO_2, USA
Electrospinning Unit	: Inovenso co., Turkey

2.3.Production of *Halomonas* Levan

Halomonas levan as an exopolysaccharide was obtained from *Halomonas* symrnensis AAD6^T (Poli, Nicolaus, Denizci, Yavuzturk, & Kazan, 2013) that was isolated form Çamaltı Saltern Area (Izmir, Turkey). The produced *Halomonas* levan was obtained by removing of bacteria from the broth using centrifugation at 10000 rpm for 20 min, then broth was removed by precipitation of levan with alcohol at a ratio of 1:1 ethanol:levan-containing-broth. The precipitate was separated from the supernatant using centrifugation at 12000 rpm for 30 min. The precipitated *Halomonas* levan was dissolved in hot distilled water for purification step that consisted of dialysis against distilled water for at least 3 days and column chromatography using a DEAE-Sepharose CL-6B.

2.4.Hydrolysis of *Halomonas* Levan

HL is a large homopolymer with an average molecular weight of 1483 kDa (Sarilmiser et al., 2015), and forms spherically symmetrical globular conformation in aqueous solutions due to extensive intermolecular hydrogen bonding (Sima et al., 2012). Hence, lowering the molecular weight of HL may help to achieve that entanglement problem and increase the solubility of the polymer as suggested by (Osman et al., 2017).

Hydrolysis of HL was performed by slightly modifying a fast and efficient microwave-assisted acid hydrolysis method (de Paula, Pinheiro, Lopes, & others, 2008) where 5% (w/v) HL in acetic acid solution was subjected to microwave irradiation for 60 secs at 60% of the maximum power of the machine. Hydrolysis products were precipitated with ethanol, dried in a vacuum oven and then milled to obtain powdered hHL samples. Thin layer chromatography (TLC) was performed by loading solutions onto lines that were drawn on thin layer plaque with the distance of 1 cm between each line. 10 mg/mL of sucrose, glucose and fructose solutions were preferred as standard samples. The used solutions contained levan, sucrose, glucose, fructose and hHL respectively. Following the

loading of solution, plaque was left for 4 hours into the tank that contained butanol, acetic acid and dH_2O with a ratio of 6:2:2. The occurred bands were observed on the dried plaque that was stained with α-naphthol.

Multi-angle laser light scattering - gel permeation chromatography (MALSS-GPC) system that was equipped with an Ultrahydrogel Linear (0.78 x 30 cm, Waters) column was used for molecular weight measurements. Analyses were done at 25°C with 0.1 M $NaNO_3$ in 2% (v/v) acetic acid mobile phase supplied to the system at a flow rate of 1.0 ml/min. The spectral analysis of hHL was performed by using Fourier transform infrared spectroscopy (FTIR) in single attenuated total reflectance (ATR) mode (JASCO 4700, USA).

2.5.Sulfation of *Halomonas* Levan

Sulfated derivatives of hHL were prepared by following a previously optimized method (Erginer et al., 2016). hHL suspension (2 %, w/v) in pyridine was stirred for 48h at room temperature. An ice bath was prepared to add 1.5 mL chlorosulfonic acid (CSA) drop wise for each gram of hHL onto hHL-pyridine solution. After stirring for 24h, saturated sodium carbonate (Na_2CO_3) solution was added to the solution for neutralization. By leaving for 24h at room temperature, phase separation was achieved. The upper phase that contains pyridine was removed by using a peristaltic pump, and the lower phase that contained sulfated polymer was dialyzed against distilled water at least 7 days. The dialyzed suspension was dried at vacuum oven, and dry sulfated hydrolyzed *Halomonas* levan (ShHL) was powdered for further processes. To determine the efficiency of sulfation process, elemental analysis of ShHL was performed by using an energy dispersive X-ray (EDX) spectroscopy on scanning electron microscope (SEM) (JEOL JSM-5910V, USA). Five different spectrum analyses were made to determine the percentage of a sulfur atom for each carbon atom.

2.6.Electrospinning process

Organic solvents are mostly preferred for synthetic polymers such as polycaprolactone (PCL) (Ahmed, Lalia, & Hashaikeh, 2015; Bhardwaj & Kundu, 2010) and in this study, PCL (10%, w/v) was dissolved in THF:DMF (1:1, v/v) solvent mixture (Croisier et al., 2012). PEO (5%, w/v) was dissolved in distilled water. ShHL (1,3,5, 7 and 10 %, (w/v))

and hHL (1,3,5, 7 and 10 %, (w/v)) were dissolved in distilled water with agitation at room temperature. A Viscometer (Brookfield, USA) and a conductivity meter (WTW Cond-3110, Germany) were used to determine viscosity and electrical conductivity of the solutions that fibrous matrices were obtained successfully.

Fibrous matrices were fabricated by co-axial electrospinning and single-needle electrospinning via a laboratory scale electrospinning unit (NS24, Inovenso co., Turkey), and the units are represented in figure 2.1, schematically. PCL+ShHL, and PEO/hHL or PEO/ShHL were used for co-axial and single needle electrospinning, respectively. The polymer solutions for each technique were placed into a 5-ml syringe and perfused by individual pumps. The co-axial electrospinning was performed with a co-axial needle where the inner diameters of inner and outer needles were 1300 μm and 2700 μm, respectively. PCL was used as core polymer while ShHL was located at the shell. The single-needle electrospinning was done with a blend of polymer solutions using a single needle that the inner diameter was 1300 μm. All experiments were carried out at ambient temperature.

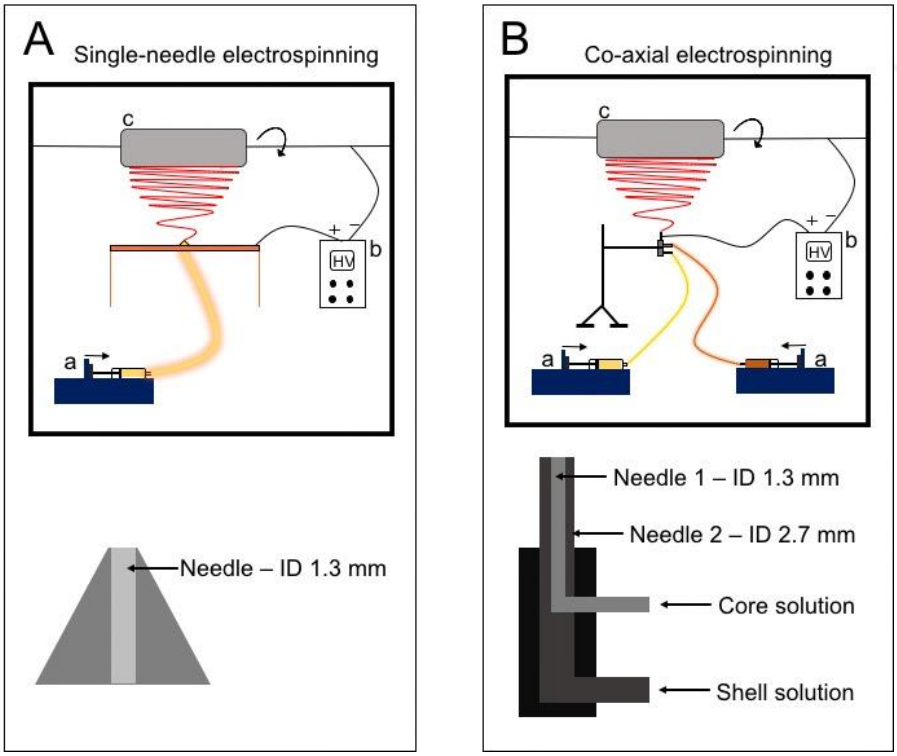

Figure 2.1: Schematic illustration of the experimental set-up of A) single-needle electrospinning and B) co-axial electrospinning processes using apparatus a) pump, b) high voltage power supply and c) collector.

2.7.Mechanical, Surface and Morphological Characterization

Samples were cut into dimensions of 3 cm x 1 cm, then the thickness of the electrospun matrices was measured by using a digital micrometer (C/N 293/100, Mitutoyo, Japan) with ±0.0001 mm accuracy. Mechanical tests were performed by recording the maximum force, elongation at break and elastic modulus during extension at 5 mm min^{-1} by Instron 4411 mechanical tester (Norwood, MA, USA) at 21ºC. Tensile strength was calculated by dividing the applied maximum force by the initial cross-sectional area of the sample. Three measurements were performed for each sample.

The surface chemistry of electrospun matrices was examined using FTIR-ATR (JASCO 4700, USA) that was equipped with a standard Ge/KBr detector. The samples were prepared by pressing the substances with the detector for FTIR spectroscopy analysis. The mid-IR region from 4000 to 400 cm^{-1} was used to collect spectra as an average of 30 scans with the resolution of 1 cm^{-1}. FTIR spectra were recorded by Spectra Manager® Suite cross-platform software that is compatible with Windows 7 Pro platform. Morphology of the fibrous matrices was observed by using JEOL JSM-5910V scanning electron microscope (SEM) at an accelerating voltage of 20 kV. Samples were cut and coated with gold (60s) before imaging. Fibrous diameters were calculated by Image J using SEM images and the histograms were obtained by using Python 3.6.0. All experiments were performed at room temperature.

2.8.Biological Characterization

2.8.1. Cell Culture

A frozen cell line vial was transferred immediately to 37ºC to apply fast thawing. When the cell solution was thawed by the percentage of nearly 80%, pre-warmed cell culture medium was added onto cell suspension drop by drop. After homogenization of the cell suspension, centrifugation at 1100 rpm for 5 min was applied to remove DMSO from the cell environment. The supernatant was discarded and the pellet was homogenized with

fresh culture medium. The cells were seeded into T25 flasks and left for incubation at 37^{o}C and 5% CO_2 containing environment.

The cells which are L929 fibroblasts and HUVECs are all adherent cells. The cell culture medium was DMEM supplemented with 10% FBS, 100 U/mL penicillin and 100 μg/mL streptomycin. The passaging of 70%-confluency-reached-cells were initiated with the trypsinization with trypsin–EDTA. Fresh cell culture medium was added onto trypsinized cell suspension to stop the activity of trypsin. The cell suspension was collected from the tissue flask and centrifuged at 1100 rpm for 5 min. After removing the supernatant, the cells were seeded into new tissue flasks according to their passage ratio with an increased passage number. After all, the cells were left into the incubator and the medium was refreshed every 2-3 days until 70% confluency was observed.

For cryopreservation, the exponentially growing cells were trypsinized and after inactivation of trypsin cell suspension was collected for centrifugation. Centrifugation was performed at 1100 rpm for 5 min. After cell counting cells were homogenized into PBS and centrifuged again at the same conditions. The cell pellet was re-suspended into the freezing solution which contained DMSO and FBS with a ratio of 1 to 9. The suspension was transferred to 1mL screw-capped cryotubes. After labeling tubes were left at -80^{o}C. It is known that DMSO is toxic to cells, because of that Thawing should be done immediately and freezing should be performed slower than thawing and fast enough to prevent any damage to cells.

2.8.2. Biocompatibility tests

All matrices were cut into square with 1 cm x 1 cm and placed into 24-well cell culture plates for biological characterization. Samples were sterilized with alcohol gradient series before rinsing with PBS for 5 times. For stabilization, samples were left in cell culture medium at 37^{o}C overnight prior to cell seeding. Mouse fibroblast cell line L929 and human umbilical vein endothelial cells (HUVECs) were seeded onto matrices at a density of $2x10^4$ cells/well for each sample. The cultures were maintained at 37^{o}C in a humidified air of 5% CO_2 incubator. The cells were seeded into tissue culture plates without any scaffold were used as the control group that the number of viable cells were 41250±760, 84940±620 and 130690±410 per well at 24h, 48h and 72h, respectively. Cell metabolic

activity on fibrous samples was examined with WST1 (4-[3-(4-iodophenyl)-2-(4-nitrophenyl)-2H-5-tetrazolio]-1,3-benzene disulfonate) cell proliferation and viability assay kit (Roche Applied Science, Germany) for 24h, 48h, and 72h. WST1 works similarly to MTT cell viability assay by reacting mitochondrial succinate-tetrazolium reductase that resulted in formazan dye. Compared to MTT, the formazan that is produced in WST1 assay is soluble in dH_2O, so the reaction product can be analyzed directly without a solubilization step. WST-1 reagent was added directly into culture after a determined culture time and incubated for 2h in 5% CO_2 humidity at 37ºC as recommended by the manufacturer. The absorbance was measured with a GloMax Multi+Microplate Multimode Reader (Promega, USA) at 450 nm. Cell viability was reported as the percentage of cell viability compared to control group that was calculated by the formula of (average of cell viability on fibrous matrices / average of control group) * 100%.

Cell biocompatibility was also visualized by DAPI staining of cells which were seeded on fibrous samples that were produced by co-axial electrospinning technique. The medium was removed from cell culture well and the fibers with cells were rinsed with PBS. 4% paraformaldehyde solution was added onto fibers and left for 30 min at room temperature. After removing the paraformaldehyde solution fibers were rinsed with ethanol solution at 70, 80 and 96% concentrations, respectively. DAPI solution was added onto fibrous matrices and left for 15 min in dark. Washing the matrices with 96% ethanol solution was done before air dry of matrices. A florescence microscope (Olympus BX51, USA) was used to observe the stained cells. All biological characterization analyses that include cell metabolic activity with WST1 assay kit and cell biocompatibility with DAPI staining were repeated three times for each sample.

2.8.3. Antithrombogenic activity

The antithrombogenic activity of PCL+ShHL matrices was determined by blood clotting test. Samples in the dimensions of 1 cm x 1 cm were heated at 38°C for 5 min in a baker. Aspirin-free fresh human blood (0.25 mL) anticoagulated with tri-sodium-citrate (in a 9:1 volumetric ratio) was dropped on the center of samples. Then 0.2 M $CaCl_2$ (0.02 mL) was added slowly to the blood droplet. Beakers were shaken gently to provide homogeneity of $CaCl_2$ and blood. The beakers were left for incubation at 38°C for 5, 15, 30 and 60

minutes, respectively. Next, 50 mL of distilled water was added into the beakers carefully. The absorbance of the supernatant at 540 nm was measured by use of a Hitachi U-1900 spectrophotometer. The beaker without any fibrous sample was used as control. Each experiment was performed in triplicate. Quantification of blood clotting index (BCI) was done by the following equation (Y. Liu, Yang, & Wu, 2010).

$$\mathrm{BCI} = \frac{\mathrm{OD}_{540\mathrm{nm}} \text{ of sample}}{\mathrm{OD}_{540\mathrm{nm}} \text{ of control group}} \times 100 \qquad (1)$$

BCI values were plotted versus time that represented the sample-blood contacting duration. As the blood clotting increases, BCI value decreases.

2.9.Statistical analysis

Statistical analyses were performed by using a single factor ANOVA followed by Tukey test using Prism 7 analysis program. Statistical significance was defined as $p<0.05$. All quantitative results are presented as the mean±std.

3. RESULTS AND DISCUSSIONS

3.1. Analytical methods on HL, hHL and ShHL

TLC was performed to visualize microwave assisted hydrolysis effect on HL. Sucrose, glucose and fructose was preferred to use as standard molecules. Figure 3.1 shows the dispersion HL molecules with different molecular weight compared to HL (showed as Lev in figure 3.1. As seen, fructose molecules also occurred during microwave assisted hydrolysis for 60 sec, but most of them are located in HL band. Hence, MALLS-GPC analysis was performed to quantify molecular weight change.

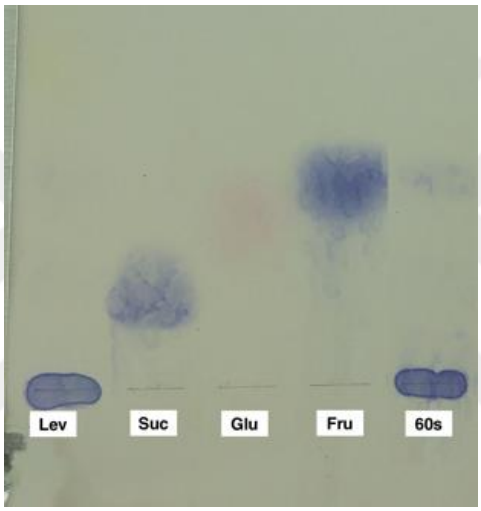

Figure 3.1: Image of TLC analysis. Lev, Suc, Glu, Fru and 60s represent HL, sucrose, glucose, fructose and hHL after 60 sec of microwave exposure.

The molecular weight of hHL was determined as 468 ± 3.4 kDa with a polydispersity of 1.221 ± 0.04 by using MALSS-GPC. The structural integrity of hHL was verified by infrared spectra recorded on a Thermo Nicolet 6700 FTIR spectrophotometer equipped with a Smart Orbit diamond ATR accessory. The typical levan peaks at 3280 cm^{-1} (-OH), 2923 and 2875 cm^{-1} (C-H), 1120, 1004 and 919 cm^{-1} (C-O-C) were observed for both HL and hHL. As seen from figure 3.2 HL and hHL had similar FTIR spectrum profile that demonstrated the structural integrity of microwave exposed hHL.

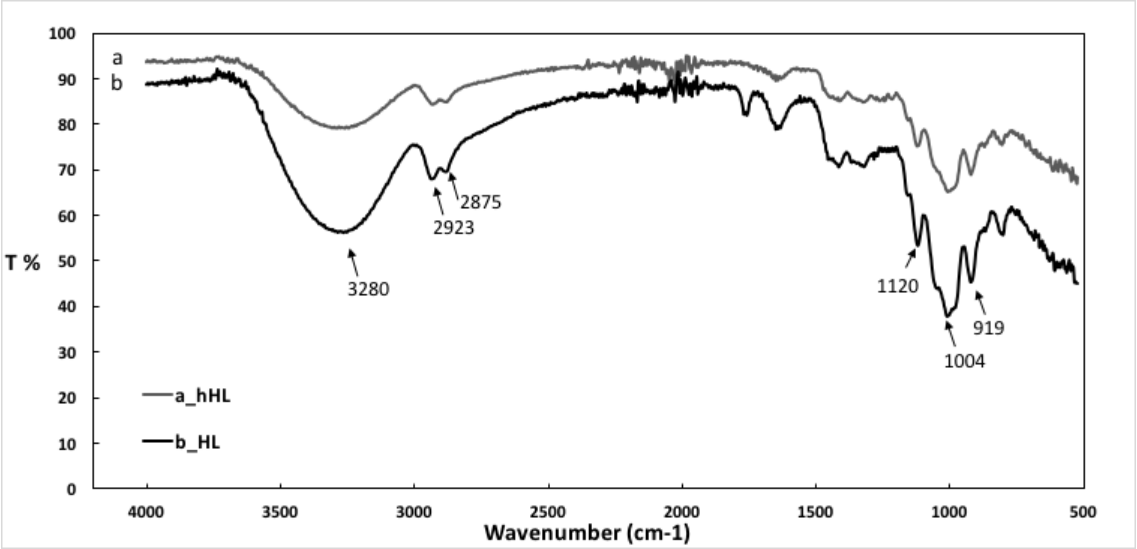

Figure 3.2: Comparative FTIR analysis results for HL and hHL

Elemental analysis of ShHL by EDX revealed a C:S atomic ratio of 6:1 which corresponded to an approximately one sulfate group for each fructose monomer along the chain and detailed characterization by 2D-NMR in a previous study revealed that hydroxymethyl groups of fructofuranose rings were the preferred site of sulfation (Erginer et al., 2016). FTIR analysis of ShHL powder showed the new bands at 1230 cm^{-1} (S=O) and 876 cm^{-1} (C-O-S) of the C-O-SO_3 groups besides the levan peaks occurred as seen figure 3.3.

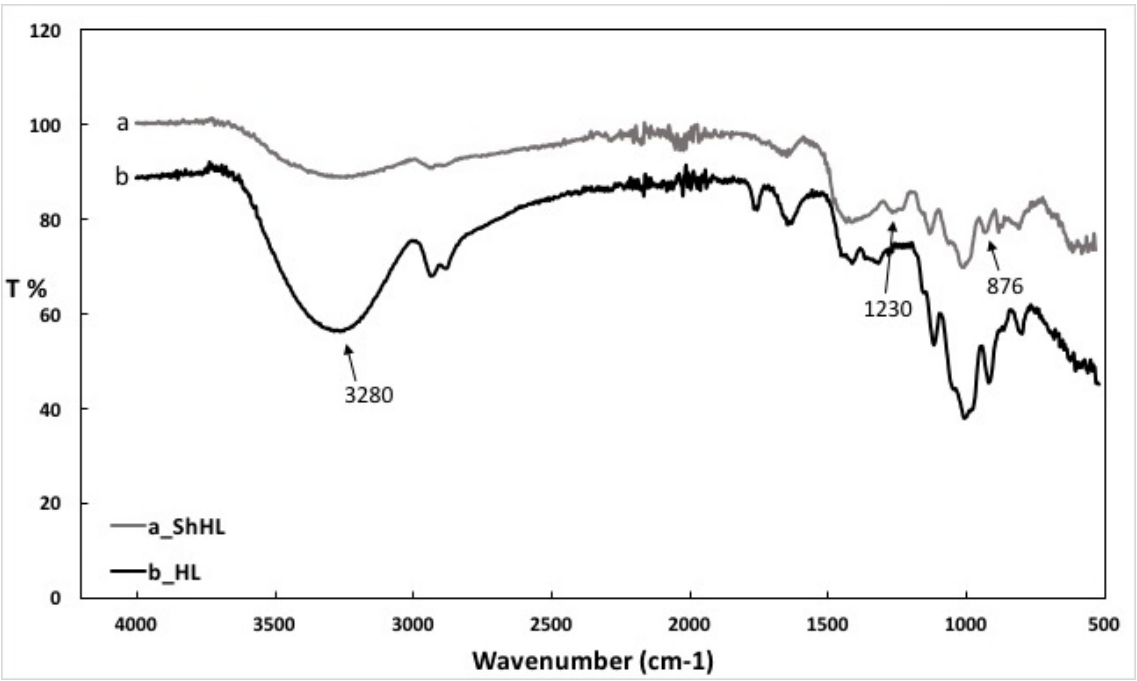

Figure 3.3: Comparative FTIR analysis results for HL and ShHL

3.2.Physical Characterization of Polymer Solutions

Viscosity, density and electrical conductivity of the electrospinning solutions are crucial physical properties that directly affect the spinning process (Kwak et al., 2017). Therefore, these physical properties of solutions used in successful electrospinning experiments were analyzed and results are shown in table 3.1. Levan is known to have a very low intrinsic viscosity when compared with other biopolymers (Freitas et al., 2011; Manandhar et al., 2009). As expected, the viscosity of ShHL increased with increasing concentration and it ranged between 2.55 mPa.s for low (1%) and 14.46 mPa.s for high (5%) concentrations, which were quite low compared with other polymers such as the alginate with 420 mPa.s viscosity (Fang, Liu, Jiang, Nie, & Ma, 2011). Similarly, hHL caused to decrease the viscosity of PEO solution to a greater extent than ShHL. The most apparent reason of an unsuccessful electrospinning is the inappropriate viscosity values that are low or high, and blending the solutions can achieve that problem by altering the viscosity to a sufficient value of 100-20000 mPa.s (Deitzel, Kleinmeyer, Harris, & Tan, 2001; J.-W. Lu et al., 2006). As seen from the table 3.1, ShHL provided sufficient viscosity values than hHL at the same concentrations.

The electrical conductivity of ShHL was higher than both PCL and PEO, and as seen, blending hHL and ShHL provided a substantial increase in electrical conductivity of PEO solutions (Table 3.1). Thinner fiber diameter is generally provided by increasing electrical conductivity, but also beads are formed due to high electrical conductivity. Instability of high conductive solutions was shown by Hayati et al., and this, in turn, results in smaller diameters and also broader diameter distributions due to bending instability (Hayati, Bailey, & Tadros, 1987; Reneker & Yarin, 2008; Yarin, Koombhongse, & Reneker, 2001). On the other hand, densities of all solutions were similar and no significant difference was observed in the density of PCL or PEO solutions with respect to their ShHL or hHL content. Increasing the concentration of ShHL and hHL to 5 % (w/v) inhibited the jet formation for single-needle electrospinning and 7 % (w/v) was the critical concentration of ShHL for co-axial electrospinning. These findings were associated with the instability in force balance between three very important parameters that are viscosity,

surface tension and conductivity as also suggested by (Cadafalch Gazquez et al., 2017; Hayati et al., 1987).

Tablo 3.1: Physical characterization of solutions used in electrospinning process

Solutions	Solvent	Electrical conductivity ($\mu S\ cm^{-1}$)	Viscosity (mPa.s)	Density (g/mL)
PCL (10%)	THF:DMF (1:1, v/v)	1.600	115	0.9382
ShHL (1%)	dH_2O	872.5	2.55	1.006
ShHL (3%)	dH_2O	2333	5.61	1.007
ShHL (5%)	dH_2O	3568	14.5	1.021
PEO (5%)	dH_2O	123.2	635	0.9600
PEO(5%)/hHL(1%)	dH_2O	170.8	305	0.9788
PEO(5%)/hHL(3%)	dH_2O	232.0	358	1.003
PEO(5%)/ShHL(1%)	dH_2O	240.0	440	1.011
PEO(5%)/ShHL(3%)	dH_2O	442.0	433	1.081

3.3.Fabrication of Electrospun Matrices

In preliminary experiments with aqueous HL and hHL solutions (up to 10%, w/v), the formation of Taylor cone without jet formation was observed, probably due to the high surface tension of HL and hHL solutions compared to other electrospinnable polymer solutions. Increasing the applied voltage caused the spray of suspension drops to the collector as also reported by (Bhardwaj & Kundu, 2010). Hence chemical modification of levan polysaccharide as well as using fiber-forming polymers (PCL and PEO) to increase the chain entanglements and decrease the surface tension of hHL and ShHL solutions were found to be necessary to obtain reproducible fibrous matrices. The solutions combinations that were successfully electrospinned have been shown in the table 3.1. Schematic explanation of electrospinning processes was shown in figure 2.1. For all spinning processes, the distance between needle and collector was kept constant at 8 cm and 12 cm for co-axial and single-needle electrospinning, respectively. The flow rate was kept at 0.6 mL/h in single-needle electrospinning for both HL and ShHL. Increase in applied voltage value was needed by increasing concentrations of hHL and ShHL. ShHL concentrations exceeding 5 % inhibited the jet formation and electrospinnability under the experimental conditions. 3 % of HL and ShHL were critical concentrations to achieve electrospinning process for formation of the jet in the given constant conditions of single-needle electrospinning. The jet formation of successful electrospinning and deformation in unsuccessful electrospinning processes were shown in figure 3.4 with the SEM images of obtained electrospun matrices. In co-axial electrospinning process, the flow of polymers was provided separately and whereas 2 mL/h was sufficient for 10% PCL, 0.7 mL/h was the starting flow rate that was reduced at lower polymer concentrations for ShHL.

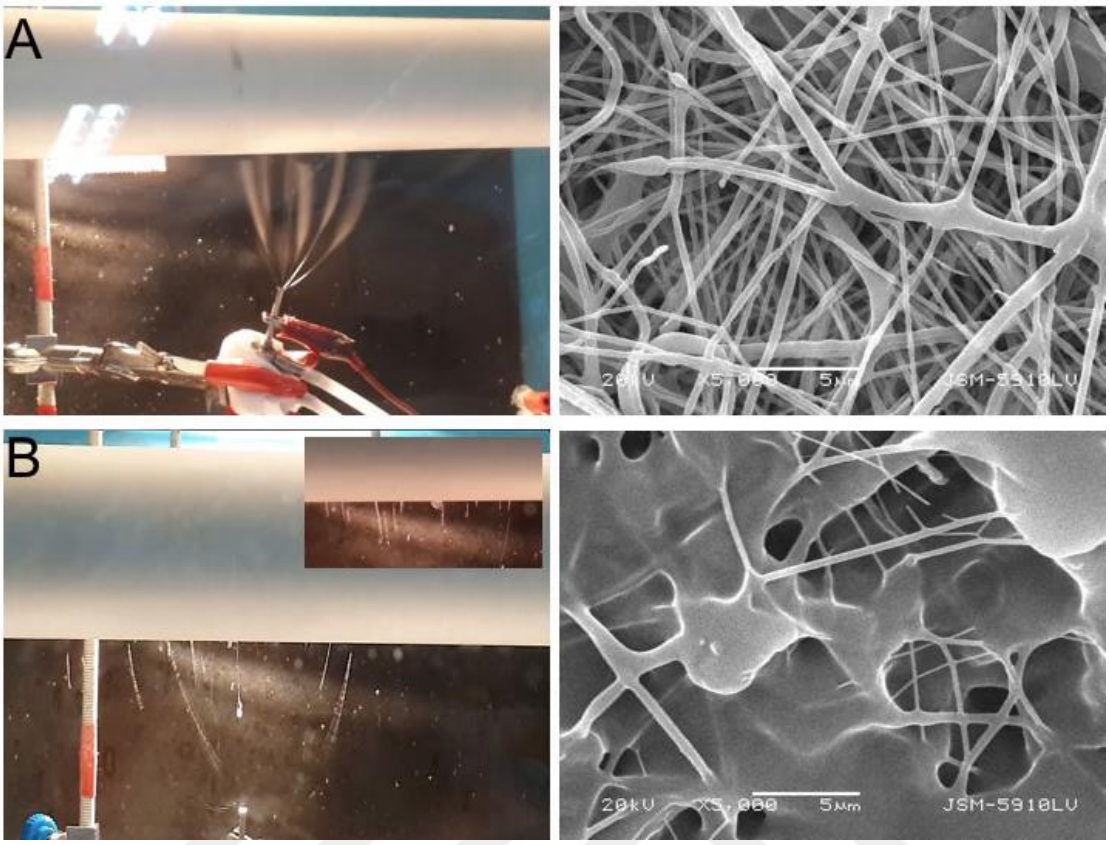

Figure 3.4: Images for A) fine fiber formation, and B) deformation in fiber formation during electrospinning process

3.4.Spectroscopic, Mechanical and Morphological Characterization of Electrospun Matrices

The infrared spectra of electrospun matrices were shown in figure 3.5. As shown in figure 3.5(A) the characteristic bands of PCL matrices were observed at 2940 cm^{-1} that referred to carbonyl stretching, symmetric CH_2 at 2864 cm^{-1}, C-C stretching at 1292 cm^{-1}, C-O stretching at 1042 cm^{-1}, and asymmetric C-O-C stretching at 1238 cm^{-1} in agreement with others (Nadri, Nasehi, & Barati, 2017; Ranjbarvan et al., 2017; Q. Zhang, Lv, Lu, Jiang, & Lin, 2015). The characteristic peaks at about 814 cm^{-1} demonstrated symmetrical C-O-S, and at about 3440 cm^{-1} indicated -OH bond of ShHL that was observed with little shifting in the fibrous matrices (Erginer et al., 2016; Shoja, Shameli, Ahmad, & Kalantari, 2015). The peaks that represented the PEO/hHL and PEO/ShHL fibers were shown in figure 3.5(B). The absorption peak at 2878 cm^{-1} corresponded to stretching vibration of C-H. C-O-C stretching peak was assigned at three peaks which were 1145, 1094 and 1059

cm^{-1}. The peaks at 1466 cm^{-1} represent CH_2 scissoring. CH_2 wagging, twisting and rocking of CH_2 were observed at 1359 and 1341 cm^{-1}, 1278 and 1240 cm^{-1}, and 960-840 cm^{-1}, respectively. The peak at 829 cm^{-1} was shown C-O-C bending (Anderson, Lamichhane, Remund, Kelly, & Mani, 2016; Gondaliya, Kanchan, Sharma, & Joge, 2011; Zebardastan, Khanmirzaei, Ramesh, & Ramesh, 2016). On the other hand, the peak for hydroxyl group at 3380 cm^{-1} was enlarged, obviously by adding of hHL and ShHL.

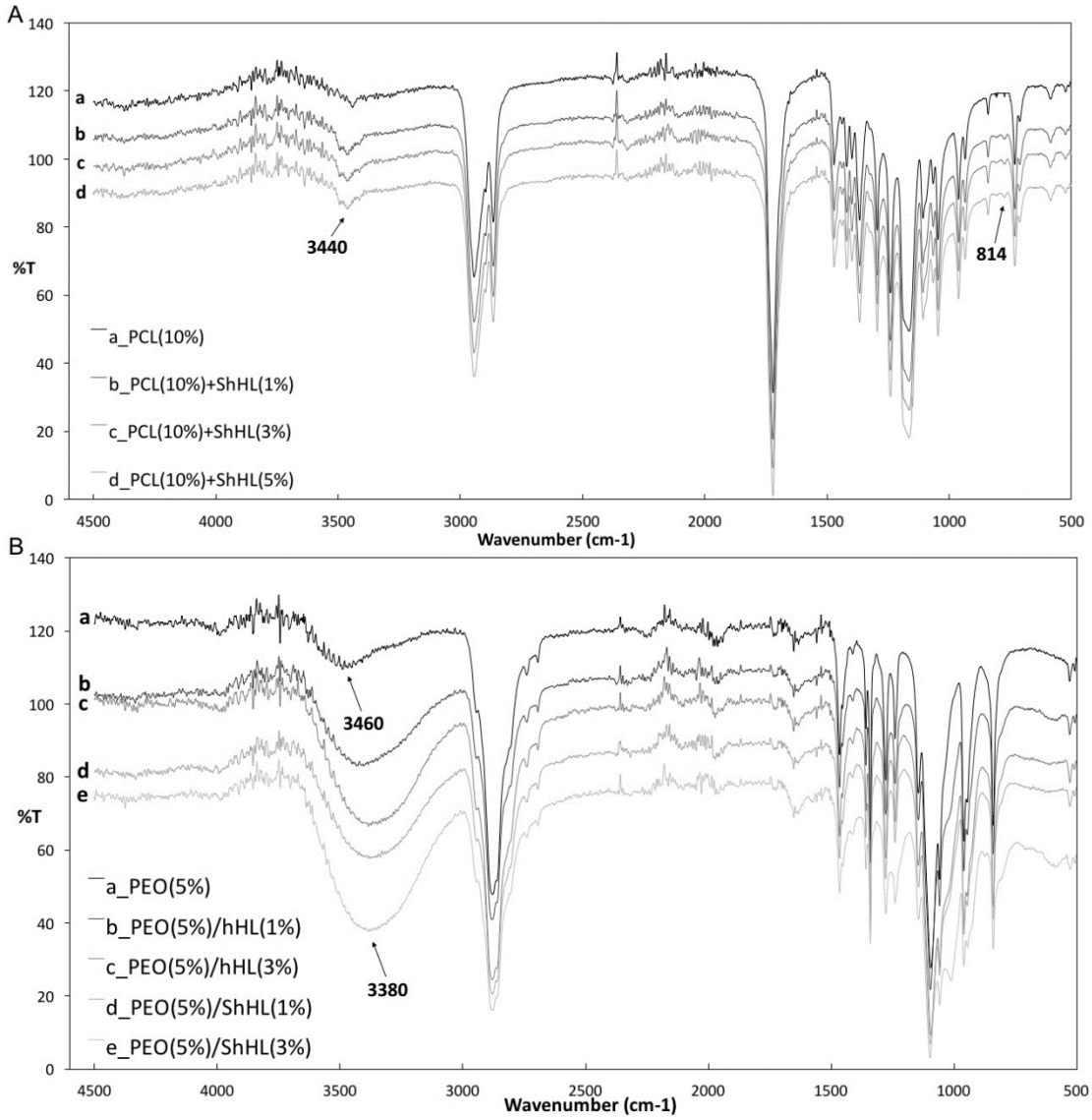

Figure 3.5: ATR-IR spectra of co-axial (A) and single-needle (B) electrospun fibrous matrices.

Tensile tests were performed to characterize the mechanical properties of the produced matrices and results are presented in table 3.2. In our previous studies with Layer-by-layer (LbL) assembled thin films, replacement of conventionally used alginate with phosphonated levan was shown to result in a three-fold improvement in lap shear adhesive strength (Costa et al., 2013). Similarly, ultimate tensile strength (UTS) of PCL matrices were found to increase with increasing ShHL concentration in the process of co-axial electrospinning. Moreover, elongation at break of PCL+ShHL matrices increased up to ten-fold when compared to PCL matrices. For the single-needle spinning, decreases were observed in the UTS such that HL blending resulted in lower UTS matrices when compared to ShHL blending. On the other hand, higher elongation at break values were obtained by blending HL and ShHL with PEO pointing to the effective energy absorbing against an applied load (Y. Z. Zhang et al., 2007). The measured thickness of electrospun matrices were 0.040 and 0.036 mm for co-axial samples and single-needle samples, respectively. It is seen that mechanical characteristics of matrices overtook properties of the porcine coronary artery that has 2.5 MPa UTS, 1 MPa modulus and 100 % elongation at break rate (Mi et al., 2016), and showed similarity with human skin that has 5-30 MPa UTS, 15-150 MPa modulus and 35-115 % elongation at break rate (Jin et al., 2013). For an unimpeded relaxation of the tissue at the end of the contraction, the low elastic modulus is desired. The material should be away from being too stiff not to restrict the contraction (Davenport Huyer et al., 2016). Ju et al reported that sheep carotid vessel has an elastic modulus of 1.53 MPa with an elongation at break of 205.35 % (Ju et al., 2017). As seen from the table the closer values were obtained with the sample of PEO(5%)/ShHL(3%), but still have nearly 4-fold higher elastic modulus. Modifying the polymer concentrations or preferring another electrospinnable polymer instead of PEO may provide similar mechanical values to native carotid vessel.

Tablo 3.2: Electrospinning parameters and mechanical properties of produced fibrous matrices

Samples	Flow rate (mL/h)	Voltage (kV)	Type of spinning	Elongation at break (%)	Elastic modulus (MPa)	Ultimate tensile strength (MPa)
PCL (10%)	2	28	Single	9.311±4.27	126.1±26.0	9.301±0.42
PCL(10%)+ ShHL(1%)	2 & 0.3*	25	Co-axial	53.93±35.8	258.2±82.0	9.958±0.72 [a]
PCL(10%)+ ShHL(3%)	2 & 0.5*	22	Co-axial	65.52±28.0 [a]	305.7±36.0	11.31±0.18 [d]
PCL(10%)+ ShHL(5%)	2 & 0.7*	20	Co-axial	94.94±26.0 [a]	279.8±72.1[a,b]	15.01±1.36 [a,b,d]
PEO (5%)	0.8	17	Single	127.1±10.6	119.0±13.71	5.318±0.04
PEO(5%)/hHL(1%)	0.6	18	Single	242.4±61.3[c]	14.85±4.70 [c]	2.858±0.02 [c]
PEO(5%)/hHL(3%)	0.6	20	Single	353.8±50.0	11.25±3.54 [c]	3.403±0.03 [c]
PEO(5%)/ShHL(1%)	0.6	20	Single	309.3±4.04 [c]	7.741±1.08 [c,e]	4.356±0.01
PEO(5%)/ShHL(3%)	0.6	23	Single	383.0±65.1[c]	5.698±0.65 [c]	4.736±0.06 [c]

[*]flow rate for ShHL polymer solution

[a]$p<0.05$ versus PCL(10%)

[b]$p<0.05$ versus PCL(10%)+ShHL(3%)

[c]$p<0.05$ versus PEO(5%)

[d]$p<0.05$ versus PCL(10%)+ShHL(1%)

[e]$p<0.05$ versus PEO(5%)/ShHL(3%)

Morphological characterization of fibrous matrices was performed with SEM imaging as seen in figure 3.6 and figure 3.7. Co-axial electrospun matrices represented as figure 3.6(A-D) showed that PCL had dense and fine fibers with minimum bead structures. The spinning of PCL with ShHL co-axially caused deformation and bead formation on the structure due to having not enough time to getting dry at the process distance. However, the fine-fiber-jet formation was not observed by increasing distance or applied voltage. That also provided the increase in fiber diameter from 2.529±1.281 μm to 2.728±1.737, 3.086±1.771, 3.373±1.831 μm with increasing ShHL concentration, respectively. Electrospun PEO matrix (Figure 3.7(A)) had a quite dense fibrous structure with an average diameter of 3.415±1.781 μm. Blending PEO with hHL or ShHL resulted in a decrease in fiber diameter. 1 and 3% (w/v) hHL blending formed fibers (Figure 3.7(B,C)) with diameters of 2.354±0.927 and 1.999±0.772 μm, respectively. ShHL blended fibrous matrices (Figure 3.7(D,E)) were observed with diameters of 0.616±0.203 and 0.390±0.157 μm for 1 and 3% (w/v) ShHL concentrations, respectively. Additionally, all average fiber diameters were represented in table 3.3.

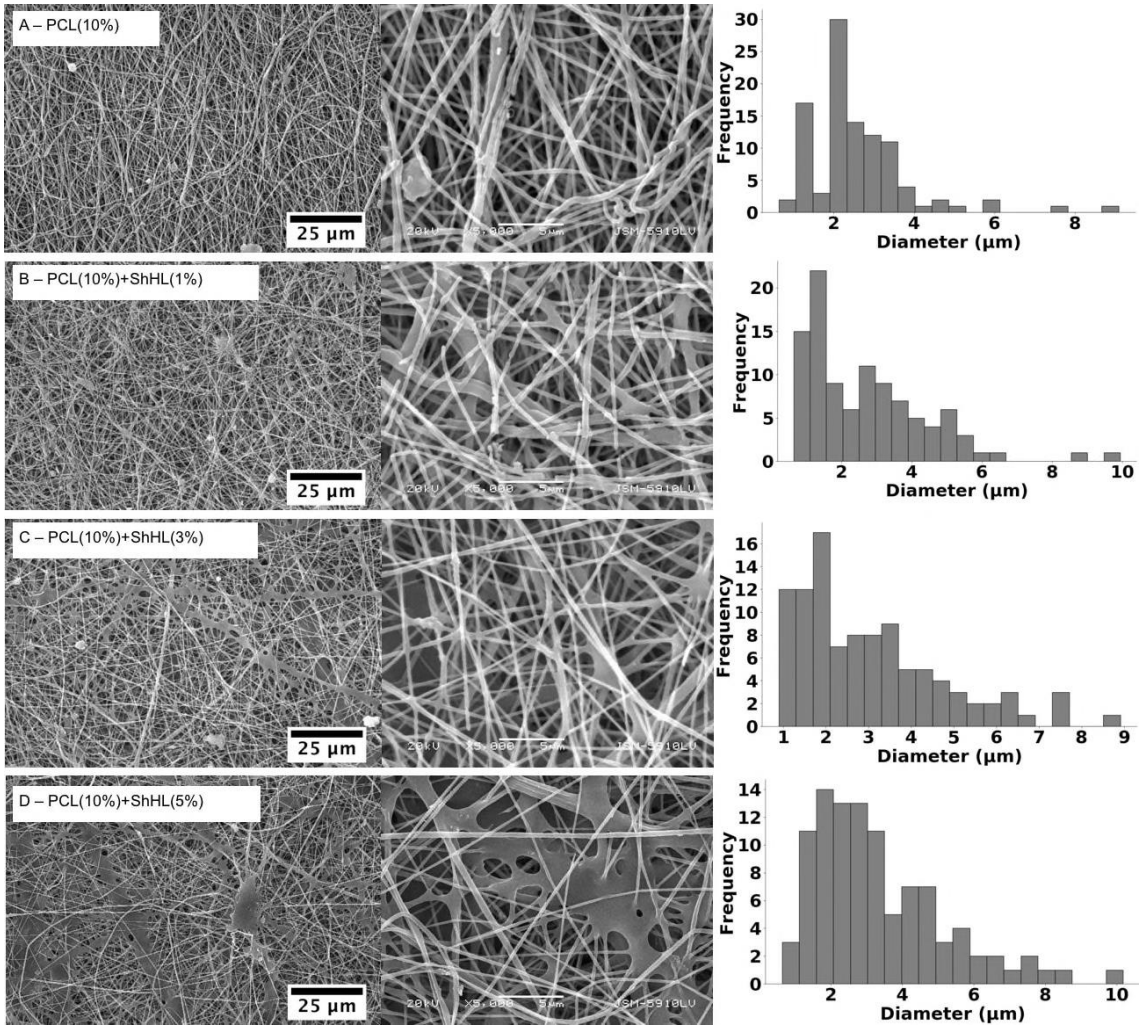

Figure 3.6: SEM images of fibrous matrices and size distribution of fibers. (A) PCL (10%), (B) PCL(10%)+ShHL(1%), (C) PCL(10%)+ShHL(3%), (D) PCL(10%)+ShHL(5%)

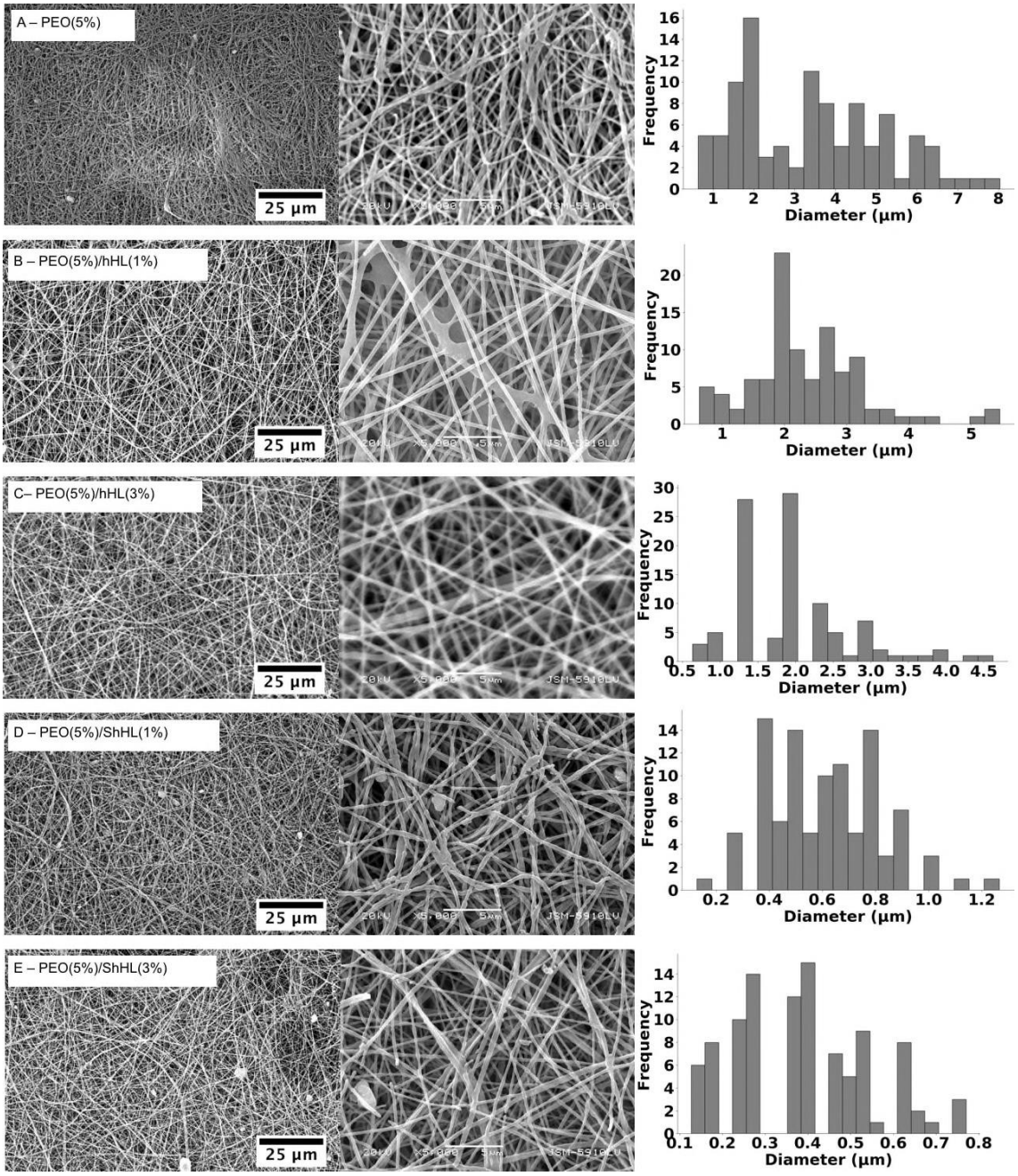

Figure 3.7: SEM images of fibrous matrices and size distribution of fibers(A) PEO (5%), (B) PEO(5%)/hHL(1%), (C) PEO(5%)/hHL(3%), (D) PEO(5%)/ShHL(1%), (E) PEO(5%)/ShHL(3%)

Tablo 3.3: Average fiber diameter of electrospun matrices

Sample	Solvent	Average fiber diameter (μm)
PCL (10%)	THF:DMF (1:1, v/v)	2.529±1.281
PCL(10%)+ ShHL(1%)	dH_2O	2.728±1.737
PCL(10%)+ ShHL(3%)	dH_2O	3.086±1.771
PCL(10%)+ ShHL(5%)	dH_2O	3.373±1.831
PEO (5%)	dH_2O	3.415±1.781
PEO(5%)/hHL(1%)	dH_2O	2.354±0.927
PEO(5%)/hHL(3%)	dH_2O	1.999±0.772
PEO(5%)/ShHL(1%)	dH_2O	0.616±0.203
PEO(5%)/ShHL(3%)	dH_2O	0.390±0.157

3.5.Biocompatibility of Fibrous Scaffolds

Heparin is known to inhibit the growth of diverse kinds of cells such as fibroblasts, vascular smooth muscle cells and mesangial cells (F. Chen et al., 2010; Del Vecchio et al., 1988). The main reason for the failure of vascular graft transplants is thrombosis that occurs after the implant surgery. Once HUVECs adhere the inner wall of vascular grafts and endothelialize, they release anticoagulant factors to prohibit platelet activation and thrombin formation (K. Liu et al., 2017; Y. Yao et al., 2014). Hence, HUVECs have a big importance by enhancing endothelialization and having direct contact with the blood. In addition, heparin-like activity with high performance is an important point for not only the materials that come across with blood but also for wound healing. In chronic wounds the healing process does not work in the same manner with normal healing process,

possibly because of rapid proteolysis of peptide growth factors. It is known that protecting several growth factors from degradation is provided by heparin, and heparin-like activity simulates re-epithelization phase in chronic skin wound healing as suggested by Kratz et al (Kratz et al., 1997). Based on the location of the injury, the proliferation of fibroblasts can be a serious problem since fibroblasts can lead to scar tissue formation that inhibits axon regeneration in spinal cord injury (Ruschel et al., 2015; Sofroniew, 2009). In this study, cellular compatibility of the scaffolds was analyzed by WST1 cell viability assay for both L929 fibroblasts and HUVECs, and the results are plotted in figure 3.8. HL is known for its supportive effect on cell proliferation (Bostan et al., 2014; Sezer et al., 2017). As seen, hHL also showed an increase in cell viability for both fibroblasts and HUVECs. On the other hand, the viability of fibroblasts on those matrices was higher than that of HUVECs reaching 159.7 % for fibroblasts and 116.1 % for HUVECs after 72 h for 3 % of hHL concentration. When hHL was compared with ShHL for HUVECs, ShHL showed higher cell viability with a ratio of 127.2 %. PEO without hHL showed nearly same results with control groups that any fibrous matrices were not used to seed the cells on. As expected, L929 fibroblast growth was inhibited in the presence of ShHL (Figure 3.8(B, D)) which was 78.7 % for co-axial electrospinning and 79.3 % for single-needle electrospinning after 72 h of cell seeding. Next, the difference of HUVECs growth at 72 h on PEO/ShHL and PCL/ShHL matrices was 4.6 % which is not significant. Cell and material biocompatibility were also analyzed via imaging cells by fluorescence staining on the fibrous matrices produced co-axially. L929 fibroblasts and HUVECs were seeded on the fibers, and at the end of 24, 48 and 72 h cells were stained with DAPI for visualization. figure 3.9 represents L929 fibroblast cell culture images, while figure 3.10 shows HUVECs on the matrices. As expected, HUVECs showed high proliferation on PCL+ShHL matrices, while cell proliferation of fibroblasts was inhibited due to the heparin-like activity of ShHL. These demonstrated results were in accordance with WST1 cell viability assay results shown in figure 3.8(A,B).

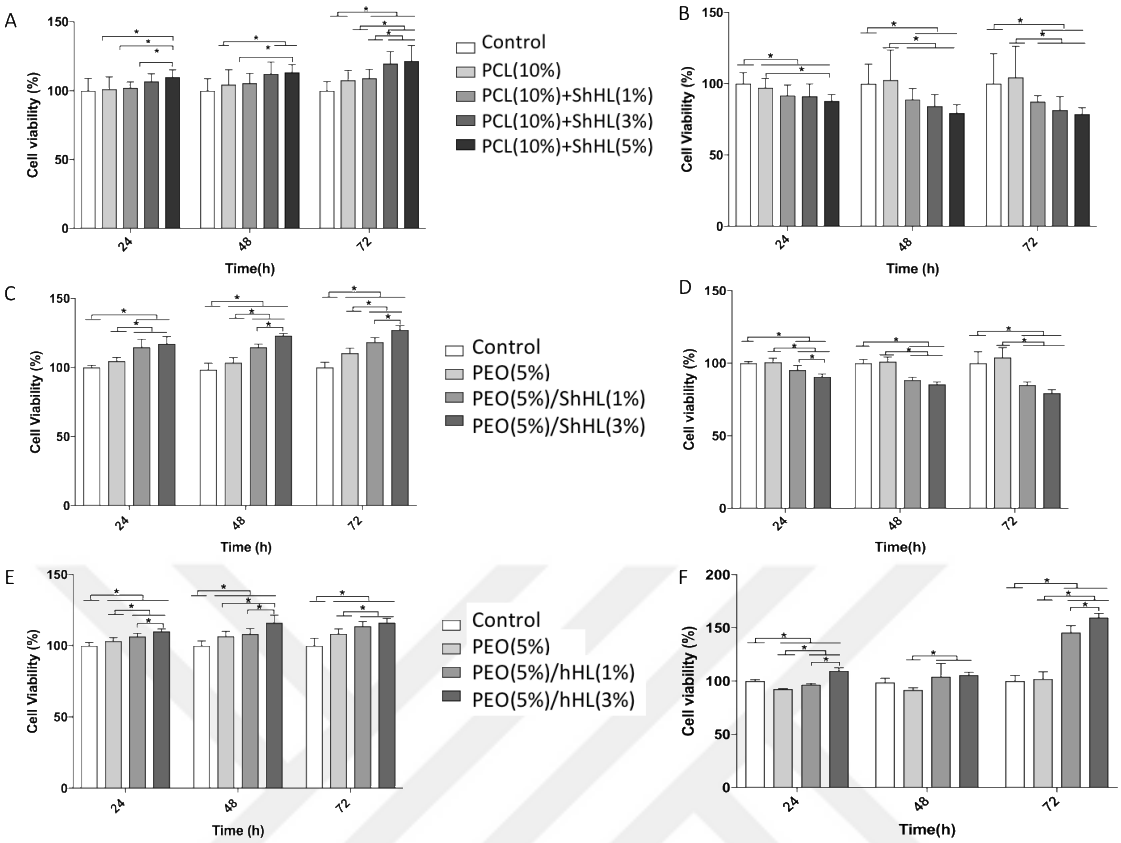

Figure 3.8: Cell viability analysis results of A) HUVECs with PCL+ShHL matrices, B) L929 fibroblasts with PCL+ShHL matrices, C) HUVECs with PEO/ShHL matrices, D) L929 fibroblasts with PEO/ShHL matrices, E) HUVECs with PEO/hHL matrices, F) L929 fibroblasts with PEO

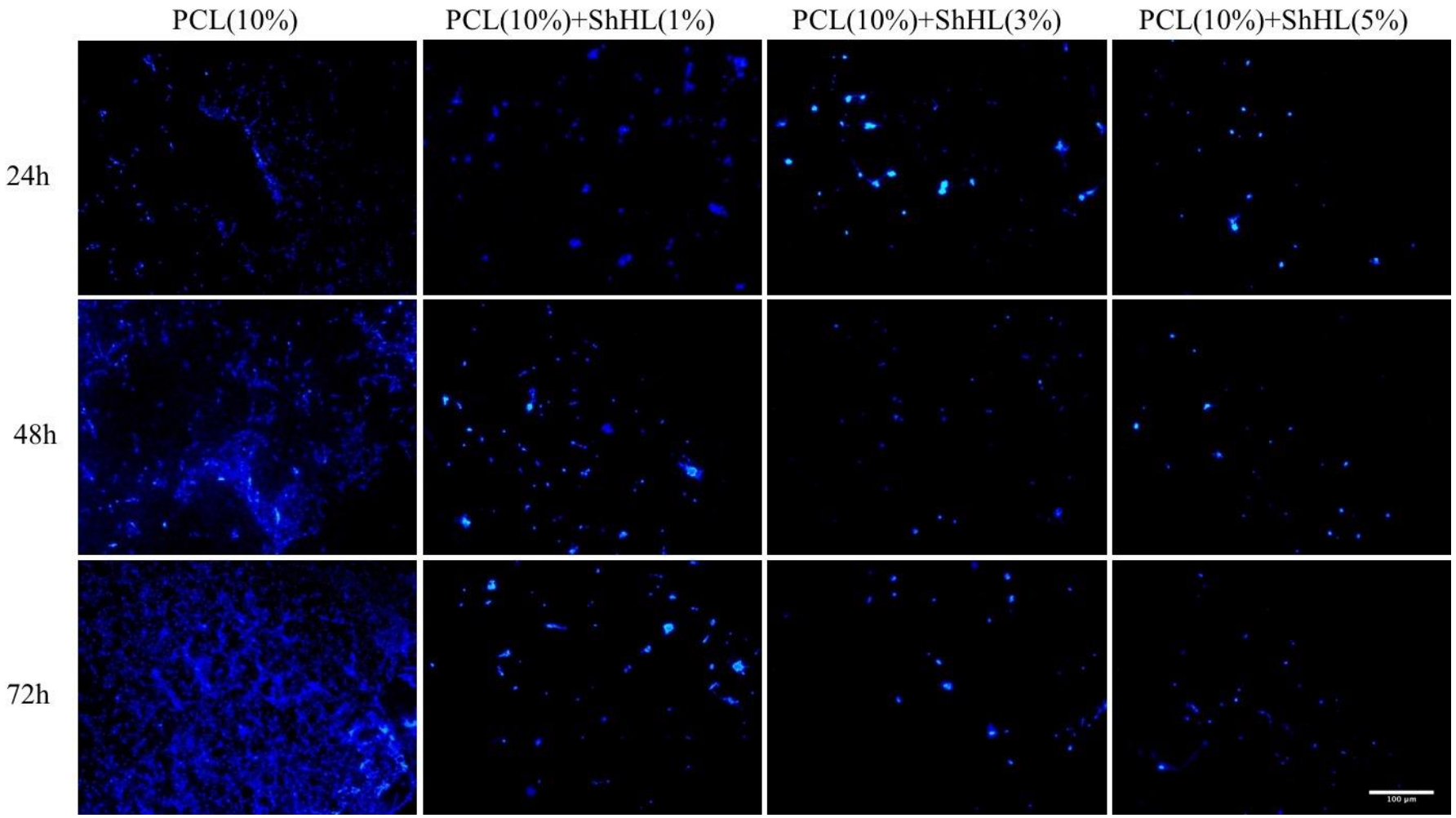

Figure 3.9: Fluorescence images of L929 fibroblasts proliferated on PCL+ShHL electrospun fibrous matrices. Scale bar of 100 µm

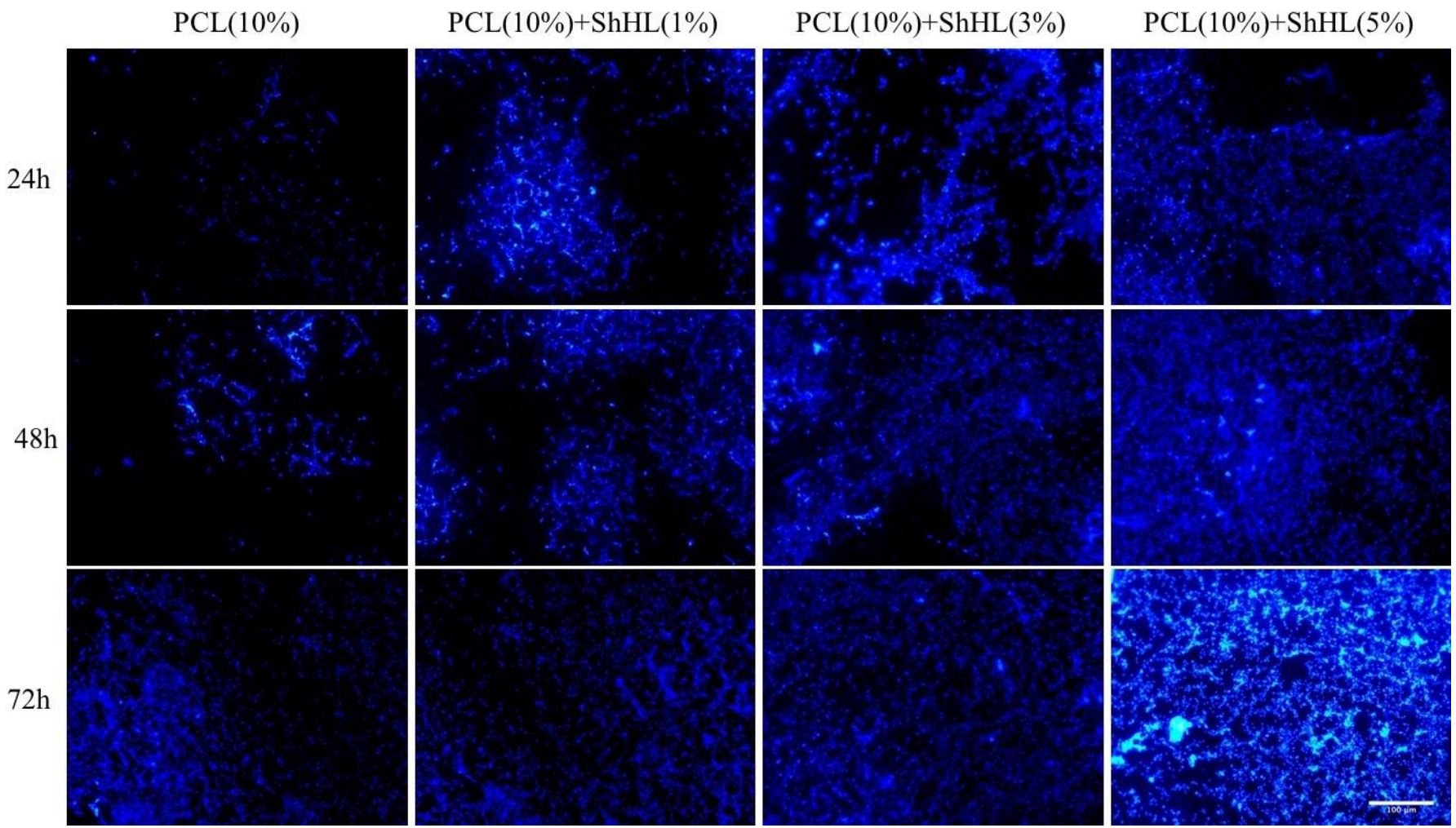

Figure 3.10: Fluorescence images of HUVECs proliferated on PCL+ShHL electrospun fibrous matrices. Scale bar of 100 µm

3.6.Antithrombogenic Properties

Antithrombogenic activity of fibrous matrices was determined by blood clotting test, and it was quantitated by the blood clotting index (BCI) that is a relative parameter. Higher BCI value represents lower thrombogenic activity that represents blood clotting. PEO/ShHL electrospun matrices have a rapid solubility property in aqueous solutions. Therefore, only PCL+ShHL fibrous matrices were used for *in vitro* blood clotting tests. As shown in figure 3.11, increasing ShHL concentration resulted in higher BCI values in determined sample-blood contact time intervals. 5% ShHL containing fibrous membrane showed four times higher BCI value (63.5) when compared with PCL-only matrices (15.9).

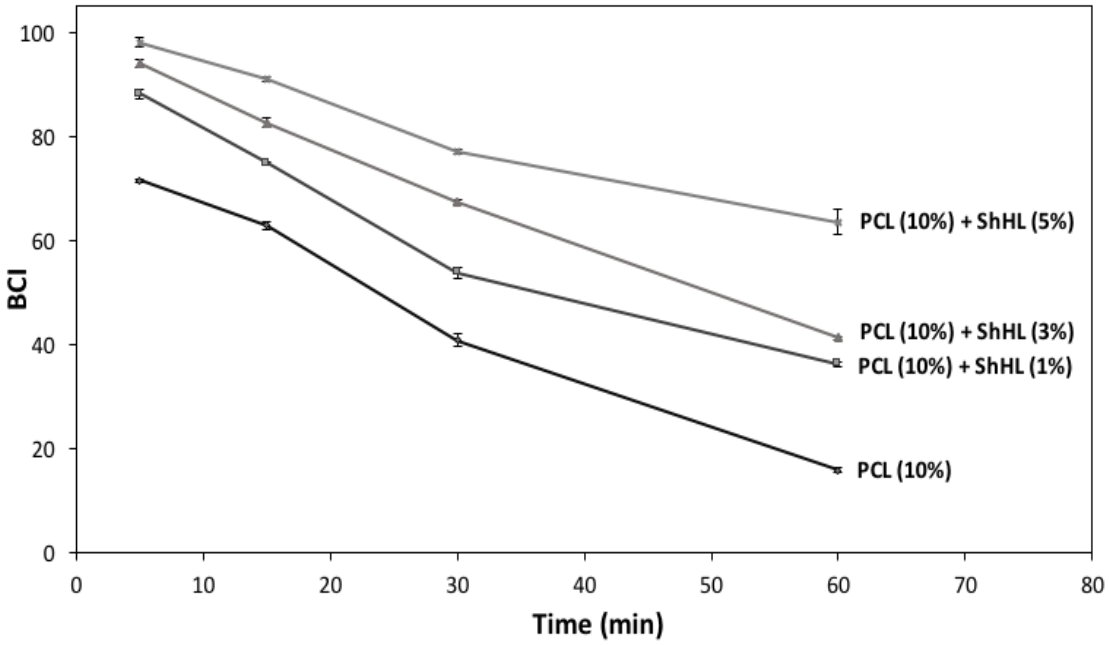

Figure 3.11: Blood clotting test of PCL+ShHL fibrous matrices with blood clotting index (BCI).

4. CONCLUSIONS AND RECOMMENDATION

Within the scope of this study, the levan polysaccharide was produced by *Halomonas smyrnensis* and fabrication of levan-based electrospun matrices were aimed. The obtained the purified *Halomonas* levan (HL) in the form of its hydrolyzed (hHL) and sulfated derivative (ShHL) were used to fabricate fibrous matrices by using single-needle and co-axial electrospinning techniques for tissue engineering applications. The analysis for characterization of fibrous matrices was performed. The electrospun matrices that are based on ShHL were investigated as a good candidate, especially for vascular tissue engineering.

Catheters, stents, and heart valves are used to treat cardiovascular diseases currently, also several synthetic materials are used in vascular bypass surgery. The main problems that are occurred after surgery are thrombosis and neointimal proliferation (Byrne, Joner, & Kastrati, 2015; van Werkum et al., 2009). Today, the most commonly used material is expanded polytetrafluoroethylene (ePTFE) graft (Lam & Wu, 2012), and novel technologies are under investigation (Mallidi & Lotfi, 2016). The implanted material must withstand physiological pressures, inhibit thrombosis and immunological response (Chang & Niklason, 2017). And levan knew with the absence of adverse medical effect as an advantage (Manandhar et al., 2009). Beside of that, sulfated derivative of levan showed heparin-like activity that provided a delay in thrombotic activity (Erginer et al., 2016). Current stent technologies may use levan-containing grafts to reduce the risk of thrombosis and prolong the graft life.

Since no levan-based electrospun matrices have been reported before, this thesis constitutes an important step toward understanding the production parameters and the characteristic of electrospun matrices, especially for tissue engineering applications. The researchers should concentrate on *in vivo* biological characterizations of electrospun matrices with respect to antithrombogenic activity and shear stress caused by body fluid.

In this thesis study, antithrombogenic activity analysis was performed just the electropun matrices that were produced from PCL and ShHL due to long degradation time in water. And PEO and ShHL containing matrices were not able to test for antithrombogenic activity analysis due to rapid degradation in the water. Since PEO, hHL, and ShHL are soluble in water, ongoing future studies are focused on using a suitable crosslinking method to prevent from rapid

degradation of these matrices in aqueous solutions for their more effective use in tissue engineering applications.

This study may be used as a reference material for levan-based fibrous matrices production for several applications that levan can be a good candidate to be used such as environmental, protective technologies, food and filtration applications besides tissue engineering applications.

REFERENCES

Abdal-hay, A., Bartnikowski, M., Hamlet, S., & Ivanovski, S. (2018). Electrospun biphasic tubular scaffold with enhanced mechanical properties for vascular tissue engineering. *Materials Science and Engineering: C*, *82*, 10–18.

Ahire, J. J., Robertson, D. D., van Reenen, A. J., & Dicks, L. M. T. (2017). Polyethylene oxide (PEO)-hyaluronic acid (HA) nanofibers with kanamycin inhibits the growth of Listeria monocytogenes. *Biomedicine & Pharmacotherapy*, *86*, 143–148.

Ahmed, F. E., Lalia, B. S., & Hashaikeh, R. (2015). A review on electrospinning for membrane fabrication: challenges and applications. *Desalination*, *356*, 15–30.

Alban, S., Schauerte, A., & Franz, G. (2002). Anticoagulant sulfated polysaccharides: Part I. Synthesis and structure–activity relationships of new pullulan sulfates. *Carbohydrate Polymers*, *47*(3), 267–276. https://doi.org/https://doi.org/10.1016/S0144-8617(01)00178-3

Ali, N., Chipara, D., Lozano, K., Hinthorne, J., & Chipara, M. (2016). Polyethylene oxide-fullerene nanocomposites. *Applied Surface Science*.

Anderson, J. A., Lamichhane, S., Remund, T., Kelly, P., & Mani, G. (2016). Preparation, characterization, in vitro drug release, and cellular interactions of tailored paclitaxel releasing polyethylene oxide films for drug-coated balloons. *Acta Biomaterialia*, *29*, 333–351.

Anton, F. (1934). Process and apparatus for preparing artificial threads. Google Patents.

Antosik, A. K., Wilpiszewska, K., & Czech, Z. (2017). Carboxymethylated polysaccharide-based films as carriers for acrylic pressure-sensitive adhesives. *International Journal of Adhesion and Adhesives*, *73*, 75–79.

Asghari, F., Samiei, M., Adibkia, K., Akbarzadeh, A., & Davaran, S. (2017). Biodegradable and biocompatible polymers for tissue engineering application: a review. *Artificial Cells, Nanomedicine, and Biotechnology*, *45*(2), 185–192.

Axente, E., Sima, F., Sima, L. E., Erginer, M., Eroglu, M. S., Serban, N., … Mihailescu, I. N. (2014). Combinatorial MAPLE gradient thin film assemblies signalling to human osteoblasts. *Biofabrication*, *6*(3), 35010.

Bacakova, L., Novotná, K., & Parizek, M. (2014). Polysaccharides as cell carriers for tissue

engineering: the use of cellulose in vascular wall reconstruction. *Physiological Research*, *63*, S29.

Basu, P., Repanas, A., Chatterjee, A., Glasmacher, B., NarendraKumar, U., & Manjubala, I. (2017). PEO–CMC blend nanofibers fabrication by electrospinning for soft tissue engineering applications. *Materials Letters*, *195*, 10–13. https://doi.org/https://doi.org/10.1016/j.matlet.2017.02.065

Berthiaume, F., Maguire, T. J., & Yarmush, M. L. (2011). Tissue engineering and regenerative medicine: history, progress, and challenges. *Annual Review of Chemical and Biomolecular Engineering*, *2*, 403–430.

Bhardwaj, N., & Kundu, S. C. (2010). Electrospinning: a fascinating fiber fabrication technique. *Biotechnology Advances*, *28*(3), 325–347.

Bikas, H., Stavropoulos, P., & Chryssolouris, G. (2016). Additive manufacturing methods and modelling approaches: a critical review. *The International Journal of Advanced Manufacturing Technology*, *83*(1–4), 389–405.

Billiet, T., Vandenhaute, M., Schelfhout, J., Van Vlierberghe, S., & Dubruel, P. (2012). A review of trends and limitations in hydrogel-rapid prototyping for tissue engineering. *Biomaterials*, *33*(26), 6020–6041.

Bostan, M. S., Mutlu, E. C., Kazak, H., Keskin, S. S., Oner, E. T., & Eroglu, M. S. (2014). Comprehensive characterization of chitosan/PEO/levan ternary blend films. *Carbohydrate Polymers*, *102*, 993–1000.

Braghirolli, D. I., Steffens, D., & Pranke, P. (2014). Electrospinning for regenerative medicine: a review of the main topics. *Drug Discovery Today*, *19*(6), 743–753.

Burton, T. P., Corcoran, A., & Callanan, A. (2017). The effect of electrospun polycaprolactone scaffold morphology on human kidney epithelial cells. *Biomedical Materials*, *13*(1), 15006.

Byrne, R. A., Joner, M., & Kastrati, A. (2015). Stent thrombosis and restenosis: what have we learned and where are we going? The Andreas Gr{ü}ntzig Lecture ESC 2014. *European Heart Journal*, *36*(47), 3320–3331.

Cadafalch Gazquez, G., Smulders, V., Veldhuis, S. A., Wieringa, P., Moroni, L., Boukamp, B. A., & ten Elshof, J. E. (2017). Influence of Solution Properties and Process

Parameters on the Formation and Morphology of YSZ and NiO Ceramic Nanofibers by Electrospinning. *Nanomaterials*, *7*(1), 16.

Calazans, G. M. T., Lopes, C. E., Lima, R., De Franc, F. P., & others. (1997). Antitumour activities of levans produced by Zymomonas mobilis strains. *Biotechnology Letters*, *19*(1), 19–21.

Casu, B., Naggi, A., & Torri, G. (2015). Re-visiting the structure of heparin. *Carbohydrate Research*, *403*, 60–68.

Chan, B. P., & Leong, K. W. (2008). Scaffolding in tissue engineering: general approaches and tissue-specific considerations. *European Spine Journal*, *17*(4), 467–479.

Chang, W. G., & Niklason, L. E. (2017). A short discourse on vascular tissue engineering. *NPJ Regenerative Medicine*, *2*(1), 7.

Chen, F.-M., & Liu, X. (2016). Advancing biomaterials of human origin for tissue engineering. *Progress in Polymer Science*, *53*, 86–168.

Chen, F., Huang, P., & Mo, X. (2010). Electrospinning of heparin encapsulated P (LLA-CL) core/shell nanofibers. *Nano Biomed Eng*, *2*(1), 84–90.

Chen, G., Guo, J., Nie, J., & Ma, G. (2016). Preparation, characterization, and application of PEO/HA core shell nanofibers based on electric field induced phase separation during electrospinning. *Polymer*, *83*, 12–19.

Chen, H., Fan, X., Xia, J., Chen, P., Zhou, X., Huang, J., … Gu, P. (2011). Electrospun chitosan-graft-poly (-caprolactone)/poly (-caprolactone) nanofibrous scaffolds for retinal tissue engineering. *International Journal of Nanomedicine*, *6*, 453.

Costa, R. R., Neto, A. I., Calgeris, I., Correia, C. R., Pinho, A. C. M., Fonseca, J., … Mano, J. F. (2013). Adhesive nanostructured multilayer films using a bacterial exopolysaccharide for biomedical applications. *Journal of Materials Chemistry B*, *1*(18), 2367–2374.

Croisier, F., Duwez, A.-S., Jérôme, C., Léonard, A. F., Van Der Werf, K. O., Dijkstra, P. J., & Bennink, M. L. (2012). Mechanical testing of electrospun PCL fibers. *Acta Biomaterialia*, *8*(1), 218–224.

da Silva, M., Martins, A., Costa-Pinto, A. R., Monteiro, N., Faria, S., Reis, R. L., & Neves, N. M. (2017). Electrospun Nanofibrous Meshes Cultured With Wharton's Jelly Stem Cell: An Alternative for Cartilage Regeneration, Without the Need of Growth Factors.

Biotechnology Journal.

Davenport Huyer, L., Zhang, B., Korolj, A., Montgomery, M., Drecun, S., Conant, G., … Radisic, M. (2016). Highly elastic and moldable polyester biomaterial for cardiac tissue engineering applications. *ACS Biomaterials Science & Engineering*, *2*(5), 780–788.

de Paula, V. C., Pinheiro, I. O., Lopes, C. E., & others. (2008). Microwave-assisted hydrolysis of Zymomonas mobilis levan envisaging oligofructan production. *Bioresource Technology*, *99*(7), 2466–2470.

Deitzel, J. M., Kleinmeyer, J., Harris, D. E. A., & Tan, N. C. B. (2001). The effect of processing variables on the morphology of electrospun nanofibers and textiles. *Polymer*, *42*(1), 261–272.

Del Vecchio, P. J., Bizios, R., Holleran, L. A., Judge, T. K., & Pinto, G. L. (1988). Inhibition of human scleral fibroblast proliferation with heparin. *Investigative Ophthalmology & Visual Science*, *29*(8), 1272–1276.

Donot, F., Fontana, A., Baccou, J. C., & Schorr-Galindo, S. (2012). Microbial exopolysaccharides: main examples of synthesis, excretion, genetics and extraction. *Carbohydrate Polymers*, *87*(2), 951–962.

Drosou, C. G., Krokida, M. K., & Biliaderis, C. G. (2017). Encapsulation of bioactive compounds through electrospinning/electrospraying and spray drying: A comparative assessment of food-related applications. *Drying Technology*, *35*(2), 139–162.

Elahi, F., Lu, W., Guoping, G., & Khan, F. (2013). Core-shell fibers for biomedical applications-a review. *Bioeng. Biomed. Sci. J*, *3*(1), 1–14.

Erginer, M., Akcay, A., Coskunkan, B., Morova, T., Rende, D., Bucak, S., … others. (2016). Sulfated levan from Halomonas smyrnensis as a bioactive, heparin-mimetic glycan for cardiac tissue engineering applications. *Carbohydrate Polymers*, *149*, 289–296.

Fang, D., Liu, Y., Jiang, S., Nie, J., & Ma, G. (2011). Effect of intermolecular interaction on electrospinning of sodium alginate. *Carbohydrate Polymers*, *85*(1), 276–279.

Fimbres-Olivarria, D., Carvajal-Millan, E., Lopez-Elias, J. A., Martinez-Robinson, K. G., Miranda-Baeza, A., Martinez-Cordova, L. R., … Valdez-Holguin, J. E. (2018). Chemical characterization and antioxidant activity of sulfated polysaccharides from Navicula sp. *Food Hydrocolloids*, *75*, 229–236.

Freitas, F., Alves, V. D., & Reis, M. A. M. (2011). Advances in bacterial exopolysaccharides: from production to biotechnological applications. *Trends in Biotechnology*, *29*(8), 388–398.

Ghasemi-Mobarakeh, L., Prabhakaran, M. P., Morshed, M., Nasr-Esfahani, M.-H., & Ramakrishna, S. (2008). Electrospun poly (-caprolactone)/gelatin nanofibrous scaffolds for nerve tissue engineering. *Biomaterials*, *29*(34), 4532–4539.

Ghosh, T., Chattopadhyay, K., Marschall, M., Karmakar, P., Mandal, P., & Ray, B. (2008). Focus on antivirally active sulfated polysaccharides: from structure--activity analysis to clinical evaluation. *Glycobiology*, *19*(1), 2–15.

Gondaliya, N., Kanchan, D. K., Sharma, P., & Joge, P. (2011). Structural and Conductivity Studies of Poly (Ethylene Oxide)--Silver Triflate Polymer Electrolyte System. *Materials Sciences and Applications*, *2*(11), 1639.

Groner, M., Ng, T., Wang, W., & Udit, A. K. (2015). Bio-layer interferometry of a multivalent sulfated virus nanoparticle with heparin-like anticoagulant activity. *Analytical and Bioanalytical Chemistry*, *407*(19), 5843–5847. https://doi.org/10.1007/s00216-015-8735-x

Gunatillake, P. A., & Adhikari, R. (2003). Biodegradable synthetic polymers for tissue engineering. *Eur Cell Mater*, *5*(1), 1–16.

Guyton, J. R., Rosenberg, R. D., Clowes, A. W., & Karnovsky, M. J. (1980). Inhibition of rat arterial smooth muscle cell proliferation by heparin. In vivo studies with anticoagulant and nonanticoagulant heparin. *Circulation Research*, *46*(5), 625–634.

Haider, A., Haider, S., & Kang, I.-K. (2015). A comprehensive review summarizing the effect of electrospinning parameters and potential applications of nanofibers in biomedical and biotechnology. *Arabian Journal of Chemistry*.

Hajiali, F., Tajbakhsh, S., & Shojaei, A. (2017). Fabrication and properties of polycaprolactone composites containing calcium phosphate-based ceramics and bioactive glasses in bone tissue engineering: a review. *Polymer Reviews*, (just-accepted), 0.

Han, Y. W., & Watson, M. A. (1992). Production of microbial levan from sucrose, sugarcane juice and beet molasses. *Journal of Industrial Microbiology & Biotechnology*, *9*(3), 257–260.

Hayashi, T. (1994). Biodegradable polymers for biomedical uses. *Progress in Polymer Science*, *19*(4), 663–702.

Hayati, I., Bailey, A. I., & Tadros, T. F. (1987). Investigations into the mechanisms of electrohydrodynamic spraying of liquids: I. Effect of electric field and the environment on pendant drops and factors affecting the formation of stable jets and atomization. *Journal of Colloid and Interface Science*, *117*(1), 205–221.

Hernandez, L., Arrieta, J., Menendez, C., Vazquez, R., Coego, A., Suarez, V., … Chambert, R. (1995). Isolation and enzymic properties of levansucrase secreted by Acetobacter diazotrophicus SRT4, a bacterium associated with sugar cane. *Biochemical Journal*, *309*(1), 113–118.

Hou, Q., Grijpma, D. W., & Feijen, J. (2003). Porous polymeric structures for tissue engineering prepared by a coagulation, compression moulding and salt leaching technique. *Biomaterials*, *24*(11), 1937–1947. https://doi.org/https://doi.org/10.1016/S0142-9612(02)00562-8

Jeong, S. I., Krebs, M. D., Bonino, C. A., Khan, S. A., & Alsberg, E. (2010). Electrospun Alginate Nanofibers with Controlled Cell Adhesion for Tissue Engineeringa. *Macromolecular Bioscience*, *10*(8), 934–943.

Jin, G., Prabhakaran, M. P., Kai, D., Annamalai, S. K., Arunachalam, K. D., & Ramakrishna, S. (2013). Tissue engineered plant extracts as nanofibrous wound dressing. *Biomaterials*, *34*(3), 724–734.

Ju, Y. M., Ahn, H., Arenas-Herrera, J., Kim, C., Abolbashari, M., Atala, A., … Lee, S. J. (2017). Electrospun vascular scaffold for cellularized small diameter blood vessels: a preclinical large animal study. *Acta Biomaterialia*, *59*, 58–67.

Kang, D. H., & Kang, H. W. (2016). Surface energy characteristics of zeolite embedded PVDF nanofiber films with electrospinning process. *Applied Surface Science*, *387*, 82–88.

Kazak, H., Barbosa, A. M., Baregzay, B., da Cunha, M. A. A., Oner, E. T., Dekker, R. F. H., & Khaper, N. (2014). Biological activities of bacterial levan and three fungal β-glucans, botryosphaeran and lasiodiplodan under high glucose condition in the pancreatic β-cell line INS-1E. *Adaptation Biology and Medicine: New Developments*, *7*, 105–115.

Kırtel, O., Avşar, G., Erkorkmaz, B. A., & Öner, E. T. (2017). Chapter 12 - Microbial

Polysaccharides as Food Ingredients. In A. M. Holban & A. M. Grumezescu (Eds.), *Microbial Production of Food Ingredients and Additives* (pp. 347–383). Academic Press. https://doi.org/https://doi.org/10.1016/B978-0-12-811520-6.00012-X

Kim, M. S., & Kim, G. (2014). Three-dimensional electrospun polycaprolactone (PCL)/alginate hybrid composite scaffolds. *Carbohydrate Polymers*, *114*, 213–221.

Knop, K., Hoogenboom, R., Fischer, D., & Schubert, U. S. (2010). Poly (ethylene glycol) in drug delivery: pros and cons as well as potential alternatives. *Angewandte Chemie International Edition*, *49*(36), 6288–6308.

Kong, L., & Ziegler, G. R. (2013). Quantitative relationship between electrospinning parameters and starch fiber diameter. *Carbohydrate Polymers*, *92*(2), 1416–1422.

Kratz, G., Arnander, C., Swedenborg, J., Back, M., Falk, C., Gouda, I., & Larm, O. (1997). Heparin-chitosan complexes stimulate wound healing in human skin. *Scandinavian Journal of Plastic and Reconstructive Surgery and Hand Surgery*, *31*(2), 119–123.

Kwak, H. W., Shin, M., Lee, J. Y., Yun, H., Song, D. W., Yang, Y., … Lee, K. H. (2017). Fabrication of an ultrafine fish gelatin nanofibrous web from an aqueous solution by electrospinning. *International Journal of Biological Macromolecules*, *102*, 1092–1103.

Lam, M. T., & Wu, J. C. (2012). Biomaterial applications in cardiovascular tissue repair and regeneration. *Expert Review of Cardiovascular Therapy*, *10*(8), 1039–1049.

Lee, H., Venable, R. M., MacKerell, A. D., & Pastor, R. W. (2008). Molecular Dynamics Studies of Polyethylene Oxide and Polyethylene Glycol: Hydrodynamic Radius and Shape Anisotropy. *Biophysical Journal*, *95*(4), 1590–1599. https://doi.org/https://doi.org/10.1529/biophysj.108.133025

Li, S., Xiong, Q., Lai, X., Li, X., Wan, M., Zhang, J., … others. (2016). Molecular modification of polysaccharides and resulting bioactivities. *Comprehensive Reviews in Food Science and Food Safety*, *15*(2), 237–250.

Li, Z., & Wang, C. (2013). Effects of working parameters on electrospinning. In *One-Dimensional Nanostructures* (pp. 15–28). Springer.

Liang, Y., & Kiick, K. L. (2014). Heparin-functionalized polymeric biomaterials in tissue engineering and drug delivery applications. *Acta Biomaterialia*, *10*(4), 1588–1600.

Liu, H., Li, X., Zhou, G., Fan, H., & Fan, Y. (2011). Electrospun sulfated silk fibroin

nanofibrous scaffolds for vascular tissue engineering. *Biomaterials*, *32*(15), 3784–3793.

Liu, J., Luo, J., Ye, H., & Zeng, X. (2012). Preparation, antioxidant and antitumor activities in vitro of different derivatives of levan from endophytic bacterium Paenibacillus polymyxa EJS-3. *Food and Chemical Toxicology*, *50*(3), 767–772.

Liu, K., Wang, N., Wang, W., Shi, L., Li, H., Guo, F., … Zhao, Y. (2017). A bio-inspired high strength three-layer nanofiber vascular graft with structure guided cell growth. *Journal of Materials Chemistry B*, *5*(20), 3758–3764.

Liu, X., & Ma, P. X. (2004). Polymeric scaffolds for bone tissue engineering. *Annals of Biomedical Engineering*, *32*(3), 477–486.

Liu, Y., Yang, Y., & Wu, F. (2010). Effects of L-arginine immobilization on the anticoagulant activity and hemolytic property of polyethylene terephthalate films. *Applied Surface Science*, *256*(12), 3977–3981.

Llorens, E., Armelin, E., del Mar Pérez-Madrigal, M., del Valle, L. J., Alemán, C., & Puiggalí, J. (2013). Nanomembranes and Nanofibers from Biodegradable Conducting Polymers. *Polymers*, *5*(3), 1115–1157. https://doi.org/10.3390/polym5031115

Loscertales, I. G., Barrero, A., Guerrero, I., Cortijo, R., Marquez, M., & Ganan-Calvo, A. M. (2002). Micro/nano encapsulation via electrified coaxial liquid jets. *Science*, *295*(5560), 1695–1698.

Lu, J.-W., Zhu, Y.-L., Guo, Z.-X., Hu, P., & Yu, J. (2006). Electrospinning of sodium alginate with poly (ethylene oxide). *Polymer*, *47*(23), 8026–8031.

Lu, Y., Wang, D., Hu, Y., Huang, X., & Wang, J. (2008). Sulfated modification of epimedium polysaccharide and effects of the modifiers on cellular infectivity of IBDV. *Carbohydrate Polymers*, *71*(2), 180–186. https://doi.org/https://doi.org/10.1016/j.carbpol.2007.05.024

Luong-Van, E., Grøndahl, L., Chua, K. N., Leong, K. W., Nurcombe, V., & Cool, S. M. (2006). Controlled release of heparin from poly (ε-caprolactone) electrospun fibers. *Biomaterials*, *27*(9), 2042–2050.

Ma, L., Deng, L., & Chen, J. (2014). Applications of poly (ethylene oxide) in controlled release tablet systems: a review. *Drug Development and Industrial Pharmacy*, *40*(7), 845–851.

Malafaya, P. B., Silva, G. A., & Reis, R. L. (2007). Natural-origin polymers as carriers and scaffolds for biomolecules and cell delivery in tissue engineering applications. *Advanced Drug Delivery Reviews*, *59*(4), 207–233.

Mallidi, J., & Lotfi, A. (2016). Late and very late stent thrombosis in the era of second generation drug-eluting stents. *EMJ*, *1*(3), 85–93.

Manandhar, S., Vidhate, S., & D'Souza, N. (2009). Water soluble levan polysaccharide biopolymer electrospun fibers. *Carbohydrate Polymers*, *78*(4), 794–798.

Manners, I. (1996). Polymers and the periodic table: recent developments in inorganic polymer science. *Angewandte Chemie International Edition*, *35*(15), 1602–1621.

Mano, J. F., Silva, G. A., Azevedo, H. S., Malafaya, P. B., Sousa, R. A., Silva, S. S., … others. (2007). Natural origin biodegradable systems in tissue engineering and regenerative medicine: present status and some moving trends. *Journal of the Royal Society Interface*, *4*(17), 999–1030.

Mi, H.-Y., Jing, X., McNulty, J., Salick, M. R., Peng, X.-F., & Turng, L.-S. (2016). Approaches to fabricating multiple-layered vascular scaffolds using hybrid electrospinning and thermally induced phase separation methods. *Industrial & Engineering Chemistry Research*, *55*(4), 882–892.

Mirjalili, M., & Zohoori, S. (2016). Review for application of electrospinning and electrospun nanofibers technology in textile industry. *Journal of Nanostructure in Chemistry*, *6*(3), 207–213.

Moghe, A. K., & Gupta, B. S. (2008). Co-axial electrospinning for nanofiber structures: preparation and applications. *Polymer Reviews*, *48*(2), 353–377.

Mondal, D., Griffith, M., & Venkatraman, S. S. (2016). Polycaprolactone-based biomaterials for tissue engineering and drug delivery: Current scenario and challenges. *International Journal of Polymeric Materials and Polymeric Biomaterials*, *65*(5), 255–265.

Mota, C., Puppi, D., Chiellini, F., & Chiellini, E. (2015). Additive manufacturing techniques for the production of tissue engineering constructs. *Journal of Tissue Engineering and Regenerative Medicine*, *9*(3), 174–190.

Nadri, S., Nasehi, F., & Barati, G. (2017). Effect of parameters on the quality of core-shell fibrous scaffold for retinal differentiation of conjunctiva mesenchymal stem cells.

Journal of Biomedical Materials Research Part A, *105*(1), 189–197.

Nigam, R., & Mahanta, B. (2014). An overview of various biomimetic scaffolds: Challenges and applications in tissue engineering. *Journal of Tissue Science & Engineering*, *5*(2), 1.

Nogueira, A. V, Drehmer, D. L., Iacomini, M., Sassaki, G. L., & Cipriani, T. R. (2017). Biological and structural analyses of bovine heparin fractions of intermediate and high molecular weight. *Carbohydrate Polymers*, *157*, 72–78. https://doi.org/https://doi.org/10.1016/j.carbpol.2016.09.061

O'brien, F. J. (2011). Biomaterials & scaffolds for tissue engineering. *Materials Today*, *14*(3), 88–95.

Oh, I.-K., Yoo, S.-H., Bae, I. Y., Cha, J., & Lee, H. G. (2004). Effects of Microbacterium laevaniformans levans molecular weight on cytotoxicity. *Journal of Microbiology and Biotechnology*, *14*(5), 985–990. Retrieved from https://www.scopus.com/inward/record.uri?eid=2-s2.0-8644284229&partnerID=40&md5=979406754ace04cf4db0f15f2f94b18b

Okutan, N., Terzi, P., & Altay, F. (2014). Affecting parameters on electrospinning process and characterization of electrospun gelatin nanofibers. *Food Hydrocolloids*, *39*, 19–26.

Oshima, T., Taguchi, S., Ohe, K., & Baba, Y. (2011). Phosphorylated bacterial cellulose for adsorption of proteins. *Carbohydrate Polymers*, *83*(2), 953–958.

Osman, A., Oner, E. T., & Eroglu, M. S. (2017). Novel levan and pNIPA temperature sensitive hydrogels for 5-ASA controlled release. *Carbohydrate Polymers*, *165*, 61–70.

Öner, E. T., Hernández, L., & Combie, J. (2016). Review of levan polysaccharide: from a century of past experiences to future prospects. *Biotechnology Advances*, *34*(5), 827–844.

Patel, H. N., Thai, K. N., Chowdhury, S., Singh, R., Vohra, Y. K., & Thomas, V. (2015). In vitro degradation and cell attachment studies of a new electrospun polymeric tubular graft. *Progress in Biomaterials*, *4*(2–4), 67–76.

Pelipenko, J., Kocbek, P., & Kristl, J. (2015). Critical attributes of nanofibers: preparation, drug loading, and tissue regeneration. *International Journal of Pharmaceutics*, *484*(1), 57–74.

Pina, S., Oliveira, J. M., & Reis, R. L. (2015). Natural-Based Nanocomposites for Bone

Tissue Engineering and Regenerative Medicine: A Review. *Advanced Materials*, *27*(7), 1143–1169.

Poli, A., Kazak, H., Gürleyenda\ug, B., Tommonaro, G., Pieretti, G., Öner, E. T., & Nicolaus, B. (2009). High level synthesis of levan by a novel Halomonas species growing on defined media. *Carbohydrate Polymers*, *78*(4), 651–657.

Poli, A., Nicolaus, B., Denizci, A. A., Yavuzturk, B., & Kazan, D. (2013). Halomonas smyrnensis sp. nov., a moderately halophilic, exopolysaccharide-producing bacterium. *International Journal of Systematic and Evolutionary Microbiology*, *63*(1), 10–18.

Ramos, P. G., Morales, N. J., Goyanes, S., Candal, R. J., & Rodr'\iguez, J. (2016). Moisture-sensitive properties of multi-walled carbon nanotubes/polyvinyl alcohol nanofibers prepared by electrospinning electrostatically modified method. *Materials Letters*, *185*, 278–281.

Ranjbarvan, P., Soleimani, M., Samadi Kuchaksaraei, A., Ai, J., Faridi Majidi, R., & Verdi, J. (2017). Skin regeneration stimulation: the role of PCL-platelet gel nanofibrous scaffold. *Microscopy Research and Technique*, *80*(5), 495–503.

Reneker, D. H., & Yarin, A. L. (2008). Electrospinning jets and polymer nanofibers. *Polymer*, *49*(10), 2387–2425.

Repanas, A., Andriopoulou, S., & Glasmacher, B. (2016). The significance of electrospinning as a method to create fibrous scaffolds for biomedical engineering and drug delivery applications. *Journal of Drug Delivery Science and Technology*, *31*, 137–146.

Ruschel, J., Hellal, F., Flynn, K. C., Dupraz, S., Elliot, D. A., Tedeschi, A., … others. (2015). Systemic administration of Epothilone B promotes axon regeneration and functional recovery after spinal cord injury. *Science (New York, NY)*, *348*(6232), 347.

Saallah, S., Naim, M. N., Lenggoro, I. W., Mokhtar, M. N., Bakar, N. F. A., & Gen, M. (2016). Immobilisation of cyclodextrin glucanotransferase into polyvinyl alcohol (PVA) nanofibres via electrospinning. *Biotechnology Reports*, *10*, 44–48.

Sachlos, E., Czernuszka, J. T., & others. (2003). Making tissue engineering scaffolds work. Review: the application of solid freeform fabrication technology to the production of tissue engineering scaffolds. *Eur Cell Mater*, *5*(29), 39–40.

Salerno, A., Netti, P. A., Di Maio, E., & Iannace, S. (2009). Engineering of foamed structures

for biomedical application. *Journal of Cellular Plastics*, *45*(2), 103–117.

Sarilmiser, H. K., Ates, O., Ozdemir, G., Arga, K. Y., & Oner, E. T. (2015). Effective stimulating factors for microbial levan production by Halomonas Smyrnensis AAD6 T. *Journal of Bioscience and Bioengineering*, *119*(4), 455–463.

Sarilmiser, H. K., & Oner, E. T. (2014). Investigation of anti-cancer activity of linear and aldehyde-activated levan from Halomonas smyrnensis AAD6 T. *Biochemical Engineering Journal*, *92*, 28–34.

Sears, N. A., Seshadri, D. R., Dhavalikar, P. S., & Cosgriff-Hernandez, E. (2016). A review of three-dimensional printing in tissue engineering. *Tissue Engineering Part B: Reviews*, *22*(4), 298–310.

Sezer, A. D., Kazak, H., Öner, E. T., & Akbu\uga, J. (2011). Levan-based nanocarrier system for peptide and protein drug delivery: optimization and influence of experimental parameters on the nanoparticle characteristics. *Carbohydrate Polymers*, *84*(1), 358–363.

Sezer, A. D., Kazak Sarilmiser, H., Rayaman, E., Çevikbas, A., Öner, E. T., & Akbuga, J. (2017). Development and characterization of vancomycin-loaded levan-based microparticular system for drug delivery. *Pharmaceutical Development and Technology*, *22*(5), 627–634.

Shao, W., He, J., Han, Q., Sang, F., Wang, Q., Chen, L., … Ding, B. (2016). A biomimetic multilayer nanofiber fabric fabricated by electrospinning and textile technology from polylactic acid and Tussah silk fibroin as a scaffold for bone tissue engineering. *Materials Science and Engineering: C*, *67*, 599–610.

Shirazi, S. F. S., Gharehkhani, S., Mehrali, M., Yarmand, H., Metselaar, H. S. C., Kadri, N. A., & Osman, N. A. A. (2015). A review on powder-based additive manufacturing for tissue engineering: selective laser sintering and inkjet 3D printing. *Science and Technology of Advanced Materials*, *16*(3), 33502.

Shoja, M., Shameli, K., Ahmad, M. B., & Kalantari, K. (2015). Preparation, characterization and antibacterial properties of polycaprolactone/ZnO microcomposites. *Digest Journal of Nanomaterials and Biostructures*, *10*(1), 169–178.

Sill, T. J., & von Recum, H. A. (2008). Electrospinning: applications in drug delivery and tissue engineering. *Biomaterials*, *29*(13), 1989–2006.

Sima, F., Axente, E., Sima, L. E., Tuyel, U., Eroglu, M. S., Serban, N., … Mihailescu, I. N. (2012). Combinatorial matrix-assisted pulsed laser evaporation: single-step synthesis of biopolymer compositional gradient thin film assemblies. *Applied Physics Letters*, *101*(23), 233705.

Sionkowska, A. (2011). Current research on the blends of natural and synthetic polymers as new biomaterials. *Progress in Polymer Science*, *36*(9), 1254–1276.

Smith, L. A., Liu, X., & Ma, P. X. (2008). Tissue engineering with nano-fibrous scaffolds. *Soft Matter*, *4*(11), 2144–2149.

Sofroniew, M. V. (2009). Molecular dissection of reactive astrogliosis and glial scar formation. *Trends in Neurosciences*, *32*(12), 638–647.

Son, W. K., Youk, J. H., Lee, T. S., & Park, W. H. (2004). The effects of solution properties and polyelectrolyte on electrospinning of ultrafine poly (ethylene oxide) fibers. *Polymer*, *45*(9), 2959–2966.

Spadaccio, C., Rainer, A., Centola, M., Trombetta, M., Chello, M., Lusini, M., … Genovese, J. A. (2010). Heparin-releasing scaffold for stem cells: a differentiating device for vascular aims. *Regenerative Medicine*, *5*(4), 645–657.

Stafiej, P., Küng, F., Thieme, D., Czugala, M., Kruse, F. E., Schubert, D. W., & Fuchsluger, T. A. (2017). Adhesion and metabolic activity of human corneal cells on PCL based nanofiber matrices. *Materials Science and Engineering: C*, *71*, 764–770.

Subramanian, A., Vu, D., Larsen, G. F., & Lin, H.-Y. (2005). Preparation and evaluation of the electrospun chitosan/PEO fibers for potential applications in cartilage tissue engineering. *Journal of Biomaterials Science, Polymer Edition*, *16*(7), 861–873.

Sultanova, Z., Kaleli, G., Kabay, G., & Mutlu, M. (2016). Controlled release of a hydrophilic drug from coaxially electrospun polycaprolactone nanofibers. *International Journal of Pharmaceutics*, *505*(1), 133–138.

Sun, B., Long, Y. Z., Zhang, H. D., Li, M. M., Duvail, J. L., Jiang, X. Y., & Yin, H. L. (2014). Advances in three-dimensional nanofibrous macrostructures via electrospinning. *Progress in Polymer Science*, *39*(5), 862–890.

Sun, Z., Zussman, E., Yarin, A. L., Wendorff, J. H., & Greiner, A. (2003). Compound core--shell polymer nanofibers by co-electrospinning. *Advanced Materials*, *15*(22), 1929–

1932.

Tos, P., Crosio, A., Pellegatta, I., Valdatta, L., Pascal, D., Geuna, S., & Cherubino, M. (2016). Efficacy of anti-adhesion gel of carboxymethylcellulose with polyethylene oxide on peripheral nerve: Experimental results on a mouse model. *Muscle & Nerve*, *53*(2), 304–309.

Vacanti, C. A. (2006). The history of tissue engineering. *Journal of Cellular and Molecular Medicine*, *10*(3), 569–576.

Van Vlierberghe, S., Dubruel, P., & Schacht, E. (2011). Biopolymer-based hydrogels as scaffolds for tissue engineering applications: a review. *Biomacromolecules*, *12*(5), 1387–1408.

van Werkum, J. W., Heestermans, A. A., Zomer, A. C., Kelder, J. C., Suttorp, M.-J., Rensing, B. J., … others. (2009). Predictors of coronary stent thrombosis: the Dutch Stent Thrombosis Registry. *Journal of the American College of Cardiology*, *53*(16), 1399–1409.

Vigneswari, S., Murugaiyah, V., Kaur, G., Khalil, H. P. S. A., & Amirul, A. A. (2016). Simultaneous dual syringe electrospinning system using benign solvent to fabricate nanofibrous P (3HB-co-4HB)/collagen peptides construct as potential leave-on wound dressing. *Materials Science and Engineering: C*, *66*, 147–155.

Wade, R. J., & Burdick, J. A. (2012). Engineering ECM signals into biomaterials. *Materials Today*, *15*(10), 454–459.

Wade, R. J., & Burdick, J. A. (2014). Advances in nanofibrous scaffolds for biomedical applications: From electrospinning to self-assembly. *Nano Today*, *9*(6), 722–742.

Wang, X., Ding, B., & Li, B. (2013). Biomimetic electrospun nanofibrous structures for tissue engineering. *Materials Today*, *16*(6), 229–241. https://doi.org/https://doi.org/10.1016/j.mattod.2013.06.005

Wang, Z., Qian, Y., Li, L., Pan, L., Njunge, L. W., Dong, L., & Yang, L. (2016). Evaluation of emulsion electrospun polycaprolactone/hyaluronan/epidermal growth factor nanofibrous scaffolds for wound healing. *Journal of Biomaterials Applications*, *30*(6), 686–698.

Williams, J. M., Adewunmi, A., Schek, R. M., Flanagan, C. L., Krebsbach, P. H., Feinberg, S.

E., … Das, S. (2005). Bone tissue engineering using polycaprolactone scaffolds fabricated via selective laser sintering. *Biomaterials*, *26*(23), 4817–4827. https://doi.org/https://doi.org/10.1016/j.biomaterials.2004.11.057

Woodruff, M. A., & Hutmacher, D. W. (2010). The return of a forgotten polymer-polycaprolactone in the 21st century. *Progress in Polymer Science*, *35*(10), 1217–1256.

Xiao, Y., Gong, T., Jiang, Y., Wang, Y., Wen, Z. T., Zhou, S., … Xu, X. (2016). Fabrication and characterization of a glucose-sensitive antibacterial chitosan--polyethylene oxide hydrogel. *Polymer*, *82*, 1–10.

Yao, Y., Wang, J., Cui, Y., Xu, R., Wang, Z., Zhang, J., … Kong, D. (2014). Effect of sustained heparin release from PCL/chitosan hybrid small-diameter vascular grafts on anti-thrombogenic property and endothelialization. *Acta Biomaterialia*, *10*(6), 2739–2749.

Yao, Z.-C., Chang, M.-W., Ahmad, Z., & Li, J.-S. (2016). Encapsulation of rose hip seed oil into fibrous zein films for ambient and on demand food preservation via coaxial electrospinning. *Journal of Food Engineering*, *191*, 115–123.

Yarin, A. L., Koombhongse, S., & Reneker, D. H. (2001). Bending instability in electrospinning of nanofibers. *Journal of Applied Physics*, *89*(5), 3018–3026.

Ye, L., Wu, X., Duan, H.-Y., Geng, X., Chen, B., Gu, Y.-Q., … Feng, Z.-G. (2012). The in vitro and in vivo biocompatibility evaluation of heparin-poly (ε-caprolactone) conjugate for vascular tissue engineering scaffolds. *Journal of Biomedical Materials Research Part A*, *100*(12), 3251–3258.

Ye, L., Wu, X., Mu, Q., Chen, B., Duan, Y., Geng, X., … Feng, Z. (2011). Heparin-conjugated PCL scaffolds fabricated by electrospinning and loaded with fibroblast growth factor 2. *Journal of Biomaterials Science, Polymer Edition*, *22*(1–3), 389–406.

Ye, Y., Ren, H., Zhu, S., Tan, H., Li, X., Li, D., & Mu, C. (2017). Synthesis of oxidized $β$-cyclodextrin with high aqueous solubility and broad-spectrum antimicrobial activity. *Carbohydrate Polymers*, *177*, 97–104.

Yu, M., Ji, Y., Qi, Z., Cui, D., Xin, G., Wang, B., … Wang, D. (2017). Anti-tumor activity of sulfated polysaccharides from Sargassum fusiforme. *Saudi Pharmaceutical Journal*, *25*(4), 464–468.

Zebardastan, N., Khanmirzaei, M. H., Ramesh, S., & Ramesh, K. (2016). Novel poly (vinylidene fluoride-co-hexafluoro propylene)/polyethylene oxide based gel polymer electrolyte containing fumed silica (SiO 2) nanofiller for high performance dye-sensitized solar cell. *Electrochimica Acta*, *220*, 573–580.

Zhang, K., Liu, Y., Zhao, X., Tang, Q., Dernedde, J., Zhang, J., & Fan, H. (2017). Anti-inflammatory properties of GLPss58, a sulfated polysaccharide from Ganoderma lucidum. *International Journal of Biological Macromolecules*.

Zhang, Q., Lv, S., Lu, J., Jiang, S., & Lin, L. (2015). Characterization of polycaprolactone/collagen fibrous scaffolds by electrospinning and their bioactivity. *International Journal of Biological Macromolecules*, *76*, 94–101.

Zhang, Y. Z., Su, B., Ramakrishna, S., & Lim, C. T. (2007). Chitosan nanofibers from an easily electrospinnable UHMWPEO-doped chitosan solution system. *Biomacromolecules*, *9*(1), 136–141.

CURRICULUM VITAE

Name Surname **:** Gülben AVŞAR

Place/Date of Birth **:** Ağrı / 04.09.1990

Foreign Language **:** English

E-mail **:** gulben.avsar@gmail.com

Education:

Degree	**University/High School**	**Department/ Program**	**Graduation Year**
High School	Sandıklı Anatolian High School	Science	2008
Bachelor of Science	Ege University	Bioengineering	2014

Presentations:

Avsar G., Gunduz O. and Öner, E. T, "Sulfated Levan Nanofibers for Biomedical Applications", "8th International Fructan Symposium", 26 June – 1 July 2016, Oaxaca/Mexico (Poster).

Avsar G., Gunduz O. and Öner, E. T, "Levan Nanofibers as Functional Biomaterials","The 3rd International Conference on Bioinspired and Biobased Chemistry & Materials", 16-19 October 2016, Nice/France (Poster).

Avsar G., Agırbaslı D., Agırbaslı M., Gunduz O. and Öner, E. T, "Co-axial and Single-Needle Electrospun *Halomonas* Levan Based Fibers for Tissue Engineering Applications","International Symposıum on Bioinspired Macromolecular Systems", 6-8 November 2017, Aveiro/Portugal (Poster)

Projects:

TUBITAK research project, "Production of Levan-Based Functional Food Ingredients" (grant number:115O495).

TUBITAK research project, "Development of Levan-Based Bioadhesive Materials" (grant number:116M838).

Publications:

Avsar G., Agırbaslı D., Agırbaslı M., Gunduz O. and Öner, E. T, Levan based Fibrous Scaffolds Electrospun via Co-axial and Single-Needle Techniques for Tissue Engineering Applications, Carbohydrate Polymers (Submitted, 2017).

Kırtel, O., Avşar, G., Erkorkmaz, B. A., and Öner, E. T.: Chapter 12 - Microbial Polysaccharides as Food Ingredients A2 - Holban, Alina Maria, pp. 347-383, in: Grumezescu, A. M. (Ed.), Microbial Production of Food Ingredients and Additives. Academic Press (2017).